REPORT DOCUMENTATION PAGE

Form Approved
OMB No. 0704-0188

Public reporting burden for this collection of information is estimated to average 1 hour per response, including the time for reviewing instructions, searching existing data sources, gathering and maintaining the data needed, and completing and reviewing the collection of information. Send comments regarding this burden estimate or any other aspect of this collection of information, including suggestions for reducing this burden to Washington Headquarters Services, Directorate for Information Operations and Reports, 1215 Jefferson Davis Highway, Suite 1204, Arlington, VA 22202-4302, and to the Office of Management and Budget, Paperwork Reduction Project (0704-0188), Washington, DC 20503.

PLEASE DO NOT RETURN YOUR FORM TO THE ABOVE ADDRESS.

1. REPORT DATE (DD-MM-YYYY)	2. REPORT TYPE	3. DATES COVERED
04-11-2003	FINAL	Jun 24,2002-Sep 30, 2003

4. TITLE AND SUBTITLE
"Artificial Muscle Technology: Physical Principles and Naval Prospects"

5a. CONTRACT NUMBER

5b. GRANT NUMBER
N00014-02-1-0778

5c. PROGRAM ELEMENT NUMBER
PR# 02 PR13092-00

6. AUTHOR(S)
Hunter, Ian W.Head PI, Professor[1]
Madden, John D.,Co-PI, Assistant Professor[2]

5d. PROJECT NUMBER

5e. TASK NUMBER

5f. WORK UNIT NUMBER

7. PERFORMING ORGANIZATION NAME(S) AND ADDRESS(ES)
[1]
Massachusetts Institute of Technology
77 Massachusetts Avenue, E19- 750(Off.Sponsored Prog.'s)
Cambridge, MA 02139, U.S.A.
[2]
University of British Columbia, Vancouver B.C. V6T 1Z3

8. PERFORMING ORGANIZATION REPORT NUMBER
MIT Off. of Spon. Res. account no.: 6893469
MIT Award #: 009419-001

9. SPONSORING/MONITORING AGENCY NAME(S) AND ADDRESS(ES)
Office of Naval Research
ONR 342, Cognitive, Neural and Biomolecular Division
800 North Quincy Street, Ballston Centre Tower One
Arlington, VA 22217-5660

10. SPONSOR/MONITOR'S ACRONYM(S)
ONR

11. SPONSOR/MONITOR'S REPORT NUMBER(S)
N00014-02-1-0778

12. DISTRIBUTION/AILABILITY STATEMENT
No limitations.

13. SUPPLEMENTARY NOTES

14. ABSTRACT
Understanding of the advantages of unsteady flow and locomotion in fish and insects is creating a demand for biomimetic actuator technologies. New actuator materials that employ voltage, field or temperature driven dimensional changes to produce forces and displacements are suggesting new approaches to propulsion and maneuverability. Fundamental properties of these new materials are presented, and examples of potential undersea applications are examined in order to assist those involved in hydrodynamic design and in actuator research to evaluate the current status and the developing potential of these artificial muscle technologies. Technologies described are based on newly explored materials developed over the past decade, and also on older materials whose properties are not widely known. The materials are dielectric elastomers, ferroelectric polymers, liquid crystal elastomers, giant magnetostrictive materials, thermal & ferroelectric shape memory alloys, ionic polymer/metal composites, conducting polymers and carbon nanotubes. Promising applications of the artificial muscle technologies are investigated in two case studies.

15. SUBJECT TERMS
linear actuators, artificial muscles, actuator descriptions, electrostrictive, electrochemical, magnetically activated shape memory alloys.

16. SECURITY CLASSIFICATION OF:			17. LIMITATION OF ABSTRACT	18. NUMBER OF PAGES	19a. NAME OF RESPONSIBLE PERSON
a. REPORT	b. ABSTRACT	c. THIS PAGE	UP	21	John D. Madden
					19b. TELEPHONE NUMBER (Include area code) 604-967-6343

Standard Form 298 (Rev. 8/98)
Prescribed by ANSI Std. Z39.18

DISTRIBUTION STATEMENT A
Approved for Public Release
Distribution Unlimited

20031126 062

FINAL TECHNICAL REPORT

GRANT #: N00014-02-1-0778

PRINCIPAL INVESTIGATOR: Ian W. Hunter, ihunter@mit.edu

INSTITUTION: Massachusetts Institute of Technology

GRANT TITLE: "Artificial Muscle Technology: Physical Principles and Naval Prospects"

AWARD PERIOD: 24 June 2002- 30 September 2003

OBJECTIVE:.
New linear actuator technologies are being developed that are of potential benefit to the Navy. These include electrostrictive materials (ferroelectric polymers, liquid crystal elastomers and dielectric elastomers), electrochemically activated materials (conducting polymer actuators, carbon nanotube actuators and ionically conductive polymer metal composites) and magnetically activated shape memory materials. The objective of this work is to provide a review of the current state of research and development in these new actuators, and an estimate of future prospects. This review provides the Navy with a basis for comparing these fledgling and disparate technologies, thereby helping identify opportunities. These opportunities include the use of artificial muscle to actuate control surfaces and propellers in order to increase maneuverability and increase stealth. Bio-mimetic propulsion schemes may also be enabled by these new technologies.

APPROACH:
Actuator technologies are compared on the bases of stress, strain, work density, power to mass, strain rate, efficiency, cycle life and cost, among other variables.

ACCOMPLISHMENTS
A comprehensive review has been assembled that is unique in its scope and quantitative approach.

CONCLUSIONS:
Several actuator technologies merit the immediate attention of the Navy. Where kilovolt level voltages are permitted, dielectric elastomers and ferroelectric polymer actuators are exciting because of their large work density (reaching 1 MJ/m^3), moderate to large strains (4-100 %) and high bandwidth (kilohertz). Where low voltages are necessary conducting polymers are preferred. However these currently suffer from relatively low bandwidth and electromechanical coupling. Vast improvements in conducting polymer molecular actuators and carbon nanotube actuators are anticipated.

SIGNIFICANCE:
Low cost and high work density actuator technologies could transform the Navy's autonomous underwater vehicle fleet by enabling greater degrees of freedom in control surfaces, improving maneuverability, reducing cost and increasing stealth.

PATENT INFORMATION:

AWARD INFORMATION:

REFEREED PUBLICATIONS (for total award period):

BOOK CHAPTERS, SUBMISSIONS, ABSTRACTS AND OTHER PUBLICATIONS (for total award period)

John D. Madden, Nate Vandesteeg, Peter G. Madden, Arash Takshi, Rachel Zimet, Patrick A. Anquetil, Serge R. Lafontaine, Paul A. Wieringa and Ian W. Hunter, "Artificial Muscle Technology: Physical Principles and Naval Prospects", *IEEE Journal of Ocean Engineering*, submitted October 2003.

John D. Madden, Nate Vandesteeg, Peter G. Madden, Arash Takshi, Rachel Zimet, Patrick A. Anquetil, Serge R. Lafontaine, Paul A. Wieringa and Ian W. Hunter, "Artificial Muscle Technology: Physical Principles and Naval Prospects", UUST Symposium, Durham New Hampshire, August 2003.

Artificial Muscle Technology: Physical Principles and Naval Prospects

John D. Madden, Nate Vandesteeg, Peter G. Madden, Arash Takshi, Rachel Zimet, Patrick A. Anquetil, Serge R. Lafontaine, Paul A. Wieringa and Ian W. Hunter

Abstract—**Understanding of the advantages of unsteady flow and locomotion in fish and insects is creating a demand for bio-mimetic actuator technologies. New actuator materials that employ voltage, field or temperature driven dimensional changes to produce forces and displacements are suggesting new approaches to propulsion and maneuverability. Fundamental properties of these new materials are presented, and examples of potential undersea applications are examined in order to assist those involved in hydrodynamic design and in actuator research to evaluate the current status and the developing potential of these artificial muscle technologies. Technologies described are based on newly explored materials developed over the past decade, and also on older materials whose properties are not widely known. The materials are dielectric elastomers, ferroelectric polymers, liquid crystal elastomers, giant magnetostrictive materials, thermal & ferroelectric shape memory alloys, ionic polymer/metal composites, conducting polymers and carbon nanotubes. Promising applications of the artificial muscle technologies are investigated in two case studies.**

I. Introduction

Electric motors, combustion engines and muscle are the dominant sources of mechanical work. The three actuator technologies are relied upon for propulsion, lifting, rotation, positioning, and the application of pressure. Piezoelectric technologies complement these actuator technologies by enabling very fine positioning at high frequencies. What is lacking is an established artificial technology that has properties similar to muscle. The properties of number of new actuators are presented that are addressing this need.

Why mimic muscle? There are no actuators that can routinely replace muscle when it fails or assist it where it is weak. Such a technology would be an enormous benefit for medical implants and human assist devices, as well as for minimally invasive surgical and diagnostic tools. Combustion engines and high revving electric motors feature high power to mass but require complex transmission systems to perform discontinuous and non-repetitive tasks, greatly reducing their efficiency and increasing cost. Direct drive electric motors are low in force and torque to mass compared to muscle. These deficiencies make human motion and dexterity nearly impossible to reproduce in robots and toys. They also make biological hydrodynamic propulsion and maneuvering strategies challenging to reproduce. It is not trivial to mimic the undulating body of a fish or create a flapping propeller blade. The availability of a muscle-like actuator will enable important advances in a number of fields.

A further drawback of electric motors and combustion engines is that, unlike most of the new technologies that are described below, they must consume energy in order to hold a load. For example, in holding a mass at a fixed height, or while generating stiffness at a fixed rudder position, electric motors expend energy, even though no mechanical work is output. In intermittent applications where minimizing energy expenditure is important, such as the positioning of control surfaces in autonomous underwater vehicle, there is substantial incentive to introduce new actuator technologies that feature a 'catch state'.

This review begins with a description of a number of actuator technologies in sequence. All technologies involve materials that change dimensions in response to input electrical, thermal or optical power. Fundamental mechanisms, basic properties, synthesis, fabrication and applications are presented. For each material a table of properties is presented. Some of the key figures of merit that are presented are now described.

Peak Stress is the maximum force per cross-sectional area that a given material is able to resist. In all the actuator technologies described, force developed scales linearly with cross-sectional area (whose surface normal is parallel to the direction in which actuation is occurring).

Materials will deform elastically in response to a change in applied load. The *Load Stress* is the maximum change in load that can be actively compensated for. It is equal to the product of the elastic modulus and the typical strain.

Strain represents the displacement normalized by the original material length in the direction of actuation. *Typical strain* is the strain that is often used in working devices, whereas *Peak strain* is the maximum strain reported.

Strain rate is average rate change in strain per unit time during an actuator stroke. Typically the maximum reported rate is given.

Manuscript received July 30, 2003. This work was supported in part by the Office of Naval Research grant N00014-1-02-0078.

J. Madden is with the University of British Columbia, Vancouver, Canada (604-827-3506; fax: 604-822-5949; e-mail: jmadden@ ece.ubc.ca). A. Takshi and P. Wierenga are also with the University of British Columbia.

N. Vandesteeg, P. Madden, R. Zimet, S. Lafontaine and I. Hunter are with the BioInstrumentation Laboratory at MIT in Cambridge MA 02139, USA.

Work Density is the amount of work generated in one actuator cycle normalized by actuator volume. It is very important to note that this does not include the volume occupied by electrolytes, counter electrodes, power supplies, or packaging, unless otherwise stated. These additional contributions to actuator volume do not always scale linearly with work output and are therefore considered separately.

Power to Mass Ratio is the peak power output per unit mass of actuator material (again only considering the material itself).

Coupling refers to the proportion of input energy that is transformed into work. This usually represents a best case, and often includes the work necessary to deform the actuator material itself.

Efficiency is the ratio of work generated to input energy expended. It can be higher than the coupling because in some cases electrical and thermal energy can be recovered from the actuator e.g. during capacitive discharge. The listed efficiency has not always been achieved in practice, and sometimes requires additional circuitry to attain. Several of the actuator technologies respond as capacitors, for example, from which electrical energy can be recovered.

Cycle Life is the number of useful strokes that the material is known to be able to undergo. Cycle life is often highly strain and stress dependent.

Elastic Modulus is the material stiffness normalized by sample length and cross-sectional area. Generally it is the instantaneous value that is reported, before any creep is induced. It is important as it determines the actuator's passive ability to reject load changes and disturbances, and along with the density & mass determines the resonant frequency. Many of these materials are viscoelastic. Creep and stress relaxation are important (but seldom characterized). Some also change stiffness with changing phase or state. Mammalian skeletal muscle changes its stiffness by a factor of 50, for example, a property that is used extensively to assist in control.

Voltage: Most of the technologies described are activated using electrical energy, which serves both to power and control the work that they generate. The *charge density* transferred, and the *dielectric constant* are also important properties.

A number of other properties are necessary in many cases to describe actuating materials including temperature dependence of the response, coefficient of thermal expansion, thermal diffusivity, ionic diffusion coefficients, resistivity, mimimum displacement, positioning resolution and gauge factor. Also environmental resistance can be important in many applications. Unfortunately these characteristics are often not known, or are not included in order to maintain a compact presentation.

The paper concludes with two case studies presenting basic design calculations relevant to the use of artificial muscle technologies to vary propeller blade camber (static) and to increase thrust by generating unsteady flow conditions. A table comparing properties of across actuator technologies is also provided.

Previous reviews include a chapter describing classical actuator technologies (electro-magnetic actuators, combustion engines, hydraulics, piezo-ceramics, muscle) by Hollerbach et. al. [1]. A review of emerging actuator technologies in comparison with muscle written by Hunter and Lafontaine over a decade ago remains relevant [2]. A book with chapters describing many of the technologies presented here, edited by Bar-Cohen, provides a comprehensive introduction [3]. Bar-Cohen also hosts an informative web site devoted to electroactive polymer actuators and devices [4]. The proceedings of the SPIE annual Smart Structures and Materials Symposium feature sessions on Electro-active Polymers, Ferroelectrics and Ferroelectric Shape Memory Alloys. Papers by Ashby and colleagues describe methods used to create a database of actuator properties [5].

II. Actuator Descriptions

A. Muscle and Biological Actuators

Muscle is a linear actuator technology whose properties, though surpassed in many respects by artificial actuators, are very well suited to providing intermittent displacements and adaptable stiffness in organisms ranging in size from the micrometer scale up to meters in length. Details of the mechanisms are provided by Kohl as part of this special issue. The properties vary by species, as described by Full and Meijer [6]. Key characteristics of mammalian skeletal muscle are provided in Table I for ready comparison with other technologies [2].

TABLE I
MAMMALIAN SKELETAL MUSCLE [2]

PROPERTY	TYPICAL	MAXIMUM
Strain (%)	20	> 40
Stress (MPa)	0.1 (sustainable)	0.35
Work Density ($kJ \cdot m^{-3}$)	0.8	
Density ($kg \cdot m^{-3}$)	1037	
Strain Rate ($\%\cdot s^{-1}$)		500
Power to Mass ($W \cdot kg^{-1}$)	50	200
Efficiency (%)		40
Cycle Life		10^9
Modulus (MPa)	10 - 60	

As mentioned, muscle does not surpass artificial actuators in any one aspect (for example continuous power to mass is an order of magnitude lower than that of an internal combustion engine). However there are a number of attractive design features that could be emulated to great advantage. For example, force can be graded by controlling the number of fibers that are activated in parallel, a process known as recruitment. This grading of force enables efficiency to be optimized over a wide range of loads and contraction velocities, in addition enabling control of acceleration and force. The control of force is made more effective by the fact that inactive muscle fibers are relatively low in stiffness, and therefore do not require significant forces to strain. In the materials described below there is little ability to change modulus. As a result attempts to grade force by recruitment are less effective. The ability to change stiffness is also

important in control strategies. For example, in catching a ball, too stiff an arm will lead to a large (painful) impulse as the ball makes contact, and provides less time to grasp the ball before it bounces back. A very compliant arm will not be able to stop the ball. The optimum stiffness needs to be adapted to the ball mass and velocity. Such stiffness control can be emulated in artificial actuators by fast feedback control, but at the expense of added complexity and only provided that the actuator bandwidth is sufficient. A further advantage of muscle is its ability to convert chemical energy to mechanical work. The 'combustion' of sugars and fats using freely available oxygen provides a fuel energy density that is two orders of magnitude greater than that of batteries. Most of the actuator technologies described below require electrical energy and will generally rely on batteries when used in autonomous systems such as AUVs. Improvement in the cost and energy density of fuel cells will alleviate this issue in systems that have access to air. Submersible use is more challenging as both fuel cells and chemical oxidation reactions require the harvesting of dissolved oxygen or of air bubbles. A further feature of muscle is its integrated circulation system, which delivers fuel (glucose and oxygen), and removes heat and waste. Capillary density is such that molecules and heat need only diffuse over distances of some tens of micrometers. Such local delivery of energy and removal of heat could greatly benefit a number of other actuator technologies. Finally, muscle is able to operate for billions of cycles over a hundred years. This exceptional performance is made possible by the ability to regenerate proteins in situ. Many of muscle's advantages relative to artificial actuator technologies stem from nature's ability to fabricate at and control on length scales ranging from the molecular to the macroscopic. As fabrication technology improves and nature's mechanisms are better understood, enormous advances will be made in actuators. Nevertheless, some newly developed artificial actuator technologies are already matching or exceeding muscle in strain, stress, and power to mass, and are thus worthy of attention.

B. Dielectric Elastomer Actuators

Mechanisms: Electrostatic attraction between conductive layers applied to two surfaces of elastomer films [7,8] induces compressive strains under applied fields of ~ 150 MV/m. Elastomers are sufficiently compliant that large strains are induced and there is efficient coupling between the electrical energy input and mechanical energy output. Typically the spacing between conductive layers is less than 0.1 mm, so that although strains are large, total displacement is small. Since elastomers maintain constant volume, contraction in one direction leads to expansion in the other two. Most mechanisms make use of the expansion perpendicular to the direction of the applied field because these result in large displacements. By pre-straining one of the two axes, all expansion is directed into the one direction. The prestraining can also result in higher breakdown potentials.

Features: The actuators are elegantly simple in mechanism and construction while featuring large strains (~100 %) and good frequency response (~ 1 kHz). High efficiencies are possible when energy is recovered (~60 %). These materials can also act as generators.

Limitations: High voltages (> 1 kV) can be a concern, particularly in biomedical and toy applications. For large and fast devices the power may provide a real hazard. Dielectric breakdown can limit actuator yield particularly when imperfections exist within films. These materials are very compliant and exhibit creep, so that although relatively large stresses can be applied (2.4 MPa), operation is more typically at ~ 100 kPa. Generally there is a need to convert line or battery voltages up to kilovolt potentials, which adds cost and consumes volume. Relatively small DC-DC converters are available for moderate to low power applications (e.g. cube 12.7 mm on each side from EMCO High Voltage), but the cost and size at present are prohibitive for application in small (e.g. handheld) portable devices [9]. Finally, the mechanisms needed to apply prestrain add significantly to volume and mass [9].

TABLE II
DIELECTRIC ELASTOMERS [8,9,10,11]

PROPERTY	SILICONE	VHB
Maximum Strain (%)	100	200
Maximum Stress (MPa)	0.4-0.8	2.4
Work Density (kJ/m^3)	1.6	58
Density (kg/m^3)	1100	960
Peak Strain Rate (%/s)	300,000	3,000
Power (W/kg)	750	3400
Bandwidth (Hz)	1400	7
Life (cycles)	10^7 (5% strain)	
Coupling (%)	6	54
Efficiency (%)	10	60
Modulus (MPa)	0.35	0.6
Speed of Sound (m/s)	18	25
Coef. Of Thermal Exp. (m/m/°C)		1.80E-04
Strength (MPa)	6.2	0.690
Voltage (V)	>1000	>1000
Charge (C/m^3)		46
Max. Field (MV/m)	110-350	125-412

Theory: The stress or pressure, P_z, resulting from electrostatic attraction between plates is:

$$P_z = \varepsilon_r \varepsilon_0 E^2 = \varepsilon_r \varepsilon_0 (V/t)^2 \qquad (1)$$

where ε_r is relative permittivity (dielectric constant), ε_0 is the free space permittivity, E is the applied electric field, V is the applied voltage and t is the thickness of the polymer. The maximum stress is limited by dielectric breakdown, which in turn is a function of strain.

In attempting to fully model this apparently simple system several complications arise. The resultant strains produced in the polymer are dependent on the boundary conditions and loads on the polymers. Further, the strain depends on the elastic modulus of the polymer, which is nonlinear at large strains. The large prestrains used can cause the effective

elastic modulus to be anisotropic. However by assuming that the elastomer is incompressible, the strains S in the x, y and z directions obey a simple relationship:

$$(1+S_x)(1+S_y)(1+S_z)=1 \qquad (2)$$

Definitely S is the relative strain, which is the strain difference from prestrain conditions.

Rate limiting factors include the inertia of the apparatus, damping within the elastomer film and the RC charging time constant.

Materials and Dimensions: A number of elastomers have been tested, with the best results achieved from three commercially available materials, namely Dow Corning HS3 silicone, Nusil CF 19-2186 silicone and 3M VHB 4910 acrylic. The silicones are cast into the desired geometry, while the VHB is purchased as an adhesive ribbon. Typical actuator dimensions before stretching are 100 μm thick, one hundred millimetres long and similar dimensions in width. These films are coated with conductive grease, powder or paint. Pre-stretching of up to 500 % is performed by rolling films, inserting them into a compliant frame or by using beams to maintain the tension. Voltage is applied to either side at voltages of up ~ 10 kV and using currents in the milliamp range.

Devices and applications: Recently "spring roll" actuators have been developed that feature up to 3 degrees of freedom each, as described in the accompanying paper in this issue by Stanford et. al. These actuators have a helical spring at their core, around which dielectric elastomer sheet is wound [9]. The sheets are coated in electrodes. In order to produce bending motions (in addition to stretching along the axis) the electrodes are patterned such that voltage can be applied independently to each of 4 sections. The resulting actuator bends in two directions and extends. This mechanism is very similar to that used in piezoceramic tube actuators, but features much larger deflections. These tubes can generate up to 30 N of force or 20 mm of displacement from a 90 mm, 18 mm diameter device. The effective stress is 0.1 MPa, and the strain is 22 %.

Demonstration devices include speakers (tweeters), and multi-legged robots [17].

Rate Limiting Mechanisms: Charging, viscoelastic behavior, resonance, dissipation induced heating and the speed of sound are all rate limiting factors.

Temperature: Dielectric elastomers have been operated successfully at 150 °C, and at –100 °C [9]. Operation below glass transition temperatures will be ineffective as the compliance will drop by two or more orders of magnitude.

Potential: Layers of thin films could enable voltage to be substantially reduced. Ideally these layers would be as thin as 100 nm, reducing potentials to the 10 V range. However this may prove difficult if even moderate strain rates are to be achieved due to the conflicting requirements that the conductivity of the electrodes be maximized and their mechanical stiffness be minimized. Increasing dielectric constant is an alternative method for reducing applied voltages, as predicted by equation (1). It may be possible to devise composite materials with high dielectric constants and moderate breakdown potentials that enable low voltage operation without sacrificing performance.

C. Relaxor Ferroelectric Polymer Actuators

Overview: The application of an electric field changes the alignment of polar groups on the polymer backbone, resulting in conformational changes and macroscopic deformation.

Features: Moderate strains are achieved (up to 5 %), with high stresses (reaching 45 MPa), good frequency response (~ 100 kHz), large work per cycle of up to 1 $MJ \cdot m^{-3}$, and high stiffness (~ 0.4 GPa). Synthesis methods are similar to those used for polyethylene, with good potential for mass production.

TABLE III
FERROELECTRIC POLYMERS [20,24]

PROPERTY	MIN	TYP	MAX
Strain (%)		3.5	5
Stress (MPa)			45
Work Density (kJ/m^3)	320		920
Density (kg/m^3)	1870		2000
Strain Rate (%/s) S3		5	
Strain Rate (%/s) S1		4.3	
Bandwidth (Hz)		5	100,000
Coupling (%) S3			0.3
Coupling (%) S1			0.45
Modulus (MPa)		400	
Voltage (V)			> 1000
Max. Field (MV/m)			150
Dielectric Constant		55	

Limitations: These actuators require high fields (~150 $MV \cdot m^{-1}$) and voltages (> 1 kV) creating the same problems outlined for dielectric elastomers. Strain decreases with frequency. Some of the fluorocarbons used in the synthesis of the materials are difficult to obtain and expensive due to environmental restrictions on their use. The process of e-beam irradiation, used in a number of the materials, is expensive and time consuming. Strain is load dependent. Electrodes applied to the surface of the polymer appear to fatigue due to the large strains imposed.

Potential: As with the dielectric elatomers, the high voltage can be reduced by using thin layers (100 nm for 15 V) or composite materials with very high dielectric constant. The relative stiffness of the electrode materials may limit the extent by which film thickness and hence applied voltage can be reduced, a limitation that might be overcome by using electrodes that are more compliant than gold and other metals commonly employed. The addition of high dielectric constant materials to the polymer matrix is showing promise in reducing the required field strength [19, 22].

Temperature: The Curie Points of many of these materials is just below room temperature. The dielectric constant and

the efficiency of coupling electrical and mechanical work is also a function of temperature.

Heat can be used instead of electrostatic energy to activate ferroelectric polymers. Heating and cooling these polymers around their Curie point produces reversible actuation (~ 10 % strain), with the coupling determined by the Carnot efficiency.

Mechanisms: Ferroelectric materials are the electrostatic analogs of ferromagnets. The application of an electric field aligns polarized domains within the material. When the applied field is removed, a permanent polarization remains. As in ferromagnets, ferroelectrics are characterized by a Curie Point, a temperature above which thermal energy prevents permanent polarization.

The ferroelectric polymer most commonly used for actuation is Poly(Vinylidene Fluoride – TriFluoroethylene). The electronegativity of the fluorine makes the polymer backbone highly polar. Local polar groups align to create polarized domains. The application of an electric field aligns polarized domains, which remain even after the field is removed. The realignment also produces reversible conformational changes which are made use of in actuation.

A key disadvantage of ferroelectric polymers is that there is substantial hysteresis. A large field must be applied in the opposite direction of the initial field in order to reverse the polarization, and substantial energy is expended, which does not produce mechanical work. The most successful materials have instead been ferroelectric relaxors in which the long range correlation between polar groups is disrupted by imperfections. These imperfections are either introduced by irradiation [20] or by the incorporation of disruptive monomers such as chlorofluoroethylene. The resulting polymers are ferroelectric relaxors, becoming paraelectric when field is removed, and displaying minimal hysteresis.

In P(VDF-TrFE) ferroelectric relaxors, application of field leads to a contraction in the direction between plates (S3), and extension perpendicular to the applied field (S1, S2). Pre-straining in one direction – e.g. S2 – enlarges the strain in the other direction – e.g. S1. The enhancement resulting from prestraining may be partly due to material anisotropies that are introduced during stretching.

Rate Limiting Mechanisms: Rates are limited by RC charging times, heating and dissipation within the materials, and resonant frequency.

D. Liquid Crystal Elastomers (LCE)

Overview: Thermal or electrostatic energy are employed to induce phase changes in liquid crystalline polymers. The changes of order and alignment of liquid crystalline side chains generate stresses in the polymer backbone, resulting in actuation. An article by Naciri et. al. in this issue presents some of the latest data on thermally actuated LCEs.

TABLE IV
LIQUID CRYSTAL ELASTOMERS [32,36,38,40]

PROPERTY	THERMAL	E-FIELD [32,40]
Strain (%)	40-45	2-4
Stress (MPa)	0.27	
Work Density (kJ/m^3)	56	
Density (kg/m^3)		
Strain Rate (%/s)	37	530
Power (W/kg)	1	
Efficiency (%)		75
Modulus (MPa)		100
Strength (GPa)		
Voltage (V)		0.11 (75 nm thick)
Max. Field (MV/m)		1.5-25
Dielectric Constant		40

Mechanisms: In 1975 de Gennes predicted that the reorientation of liquid crystal molecules during a phase transition could lead to a mechanical stress and strain. Stress fields in normal liquid crystals generally induce flow that prevents the buildup of a static stress. In liquid crystal elastomers, the free flow of the liquid crystal molecules (mesogens) is prevented by bonding them to a cross-linked polymer where the flexible polymer backbone still allows reorientation of the mesogens. The change in orientation of the mesogens upon temperature changes or application of an electric field can then produce stresses and strains that are transferred via the polymer to do mechanical work. Note that mechanisms of actuation in LCEs are very similar to the ferroelectrics described above, with the exception that the polarized units do not form part of the polymer backbone itself, but rather are appendages extending from it.

Rate is limited by heat transfer time constants when thermally driven. For a step change in temperature applied to the surface of a thin film of material, an estimate of the time constant of the diffusive heat transfer within the polymer itself can be given as:

$$\tau = R_{th} \cdot C_{th} = \rho \cdot C_v \cdot L^2 \qquad (3)$$

where $R_{th} = \rho \cdot L / A$, $C_{th} = C_v \cdot L \cdot A$, and ρ is the thermal resistivity, C_v is the volumetric heat capacity, A is the area perpendicular to the heat flow, and L is the distance the heat must diffuse. The quantity $(\rho \cdot C_v)^{-1}$ is known as the thermal diffusivity. Leister et al. [33] measured the thermal diffusivity for a ferroelectric liquid crystalline elastomer with a polysiloxane backbone and found values of 2×10^{-8} to 4×10^{-8} m^2/s. For a flat film with a thickness of 100 μm, the corresponding time constant is between 0.25 and 0.5 s. The rate is expected to be proportional to the inverse square of thickness, so it should be possible to activate a 1 μm thick film in less than 100 μs.

Ferroelectric liquid crystals contract and expand when an external electric field is applied to the polymer [32,40]. The mesogenic units in ferroelectric liquid crystals have an intrinsic polarization. The application of the field changes the alignment of the mesogens and, if they are attached to a polymer backbone, can induce bulk stressses and strains.

Unlike thermal energy, electric fields can be applied through the bulk of the material very quickly, so the response speed is considerably faster in electrostatic-driven films than

during thermally induced activation. The time taken to reorient the liquid crystal units is the ultimate rate-limiting factor in ferroelectric liquid crystalline elastomers. In experiments designed to determine the speed to the mesogenic reorientation, Skupin, et al. [37] used time resolved FTIR to measure a response of ~ 10 ms. It should be expected that the response time depends greatly on the specific mesogens used, the polymer backbone structure, and the degree of cross-linking.

In separate experiments by the same group [32], 4% electrostrictive strains were observed in a ferroelectric liquid crystalline elastomer at 133 Hz. In these experiments an electric field of 1.5 MV/m was applied to a thin (75 nm) microtomed sample. Results at other excitation frequencies were not presented and so it is not clear what the frequency dependence of the response looks like. Recent experiments by Zhang and colleagues [40] show a 2 % strain at 25 $MV \cdot m^{-1}$ in a relatively stiff material, but also an apparently rapid drop off in frequency response above 1 Hz.

The low stiffness of these materials means that resonant frequencies will also tend to be low.

Features: These materials exhibit fast response times (~10 ms by field driven actuation [32]), and moderate to large strains. The applied fields (1.5 MV/m) are lower than those used in other ferroelectrics and in dielectric elastomers, leading to correspondingly lower applied voltages for the same thickness of material.

These materials can also be activated via radiative heating, which can potentially create fast activation in one direction, providing absorption can be made uniform (cooling will still rely on thermal conduction) [36].

Limitations: Investigation of LCEs is still at a very early stage with the result that much information has yet to be collected. These materials are elastomers with low stiffness and tensile strength so that a relatively small change in load can easily lead to a large change in length. Thermal activation is limited by Carnot efficiency, and heating must continue during activation periods (unless cooling can be turned on and off). The rate of thermal actuation is limited by heat transfer rates. Very fast rates might be achieved using an laser heating, but at the cost of further reduced efficiency.

E. Conducting Polymer Actuators

Synonym: Conjugated polymers

Mechanisms: Conducting polymers are electronically conducting organic materials. Electrochemically changing oxidation state leads to addition or removal of charge from the polymer backbone and a flux of ions to balance charge. This ion flux, which can be accompanied by solvent, is associated with swelling or contraction of the material [41-44]. Insertion of ions between polymer chains appears to be primarily responsible for dimensional changes, although conformational changes of the backbone may also play a role. Changes in dimension can also be chemically triggered [44].

Features: High tensile strengths (120 MPa), stresses (up to 34 MPa [45]) and stiffnesses (~ 1 GPa modulus [46-48]), combined with low voltages (~ 2 V) make this actuator technology attractive.

Limitations: The electromechanical coupling in these materials is often less than 1 % [48,49]. As a result, efficiency is also low unless a substantial portion of the input energy is recovered. A consequence of the low electromechanical coupling and the low activation voltages is that very high currents can be required to operate at high power [46], putting constraints on the power supply. Encapsulation issues need to be addressed in order to isolate actuators from the environment. The moderate strains (~2 %) require mechanical amplification in most applications.

Modeling: Experiments show that strain, ε, is proportional to the density of charge, ρ, transferred over a range of strains of about 0.5 %:

$$\varepsilon = \frac{\sigma}{E} + \alpha \cdot \rho \qquad (3)$$

where σ is the applied stress and E is the elastic modulus [41,42,46-49]. The strain to charge ratio, α, is typically in the range of $\pm 1\text{-}3\times10^{-10}$ $m^3 \cdot C^{-1}$ [48]. The sign of the strain to charge ratio is negative when cations dominate the ion transfer and positive when it is anions that serve to balance charge [42]. The ion that dominates is generally the smallest of the available cations and anions. For larger strains this relationship continues to hold to first order. At stresses of more than 5 MPa, effects of creep and stress relaxation begin to become significant, and so the purely elastic model is no longer sufficient [45].

If the strain to charge ratio is re-expressed in terms of change in volume per ion transferred, the volume corresponds approximately to the size of an ion [48]. However, the correlation between ion size and strain to charge ratio is weak [50].

TABLE V
CONDUCTING POLYMER ACTUATORS

PROPERTY	MIN.	TYP.	MAX.	LIMIT	REFS.
Strain (%)		2	30		46,47
Stress (MPa)		5	34	200	41,45-47
Work Density (kJ/m^3)		100			46
Strain Rate (%/s)		1	12		55,56
Power (W/kg)			150		
Life (cycles)		28000	800000		55
Coupling		0.1	1		48
Efficiency (%)		0.1	18	100?	48
Modulus (GPa)	0.2	0.8	3		46,48,52,55
Tensile Strength (MPa)		30	120		48
Applied Potential (V)	0.1	1.2	10		56
Charge Transfer (C/m^3)	10^7		10^8		46-49
Conductivity (S/m)		10,000	45,000		48,54
Cost (US$/kg)	3		1000		48

Rate of actuation is primarily limited by the rate at which charge can be injected. Charge transfer is restricted by the internal resistance of the cell and by the rate at which ions are

transferred within the polymer [46]. The fastest response is observed in thin films with closely spaced electrodes that employ highly conducting polymer.

Materials and Dimensions: Polypyrrole and polyaniline are the most widely used materials. There has also been some use of polyacetylenes [51], polythiophenes and polyethyldioxithiophene [59]. Monomers are available (e.g. www.aldrich.com, www.basf.com) for these materials. The most common mode of synthesis is electrodeposition, producing thin (~40 μm thick) films with typical widths of 10 mm and lengths of up to 1 m or more [48]. They can also be electrodeposited as tubes [52], or chemically synthesized [44,53]. The properties of the polymers are very dependent on the solvent and salts used in deposition [54], and also the electrolyte employed during actuation [42,47,55]. The life for example can be extended to at to least one million cycles from several tens of thousands by using ionic liquid electrolytes [55].

Forces produced by actuators have reached tens of Newtons with displacements of several millimeters and use of mechanical amplification increases displacements up to about 100 mm [60]. Voltages of up to 10 V are used to drive currents that reach several hundred milliamperes. Voltages of only 1-2 V are sufficient for activation, but higher voltages help speed actuation [56]. At steady state (no motion) current is minimal, even when forces are applied.

Temperature: Little work has been done to characterize the response of conducting polymer actuators under conditions other than room temperature. Changes in the creep behavior between body temperature and room temperature have been reported. Also, the conductivity of the polymer is known to be a function of temperature and synthesis conditions [57,58]. Polymers that exhibit a large temperature dependence of conductivity will be slower at low temperatures due to the increase in internal resistance. Electrolyte conductivity and ion diffusion rates are anticipated to decrease in proportion to the square root of absolute temperature, thereby affecting rates at low temperatures. Finally, solvents and electrolyte freezing will drastically reduce rate. Typical freezing temperatures are between –60°C and 0°C.

Applications: Demonstration braille cells [55] and variable camber blades have been built [60]. On the micro-scale cell traps, and medical devices are being created [61].

Potential: Layers of thin porous films could enable extremely fast, high power response (> 100 kW/kg). Recovery of stored electrochemical energy should enable moderate efficiencies to be achieved even at full strain (> 10 %). Newly designed conducting polymers promise larger strains and higher electromechanical coupling, but are still at an early stage of development (see next section).

References:

F. Molecular Actuators

Mechanism: Electrochemically or chemically activated single polymers molecules whose molecular structure reversibly changes conformation, leading to mechanical deformations as charge is added or removed. Work is performed from the molecular level up, leading to displacement and performance from the microscopic to macroscopic level. These materials are still at an early stage of development.

Features: These materials operate at low voltages (~ 2 V), and exhibit large strains (>20 %). They are expected to achieve high efficiencies and stresses [71].

Theory: Molecular conformational changes are induced in materials designed to utilize a variety of molecular mechanisms such as the *cis-trans* photoactivated transition, molecular bending in thianthrene or π–π molecular dimerization [62-65]. In principle, the molecular structure is organized in order to maximize displacement and efficiency.

Example: Poly(calix[4]arene bis-bithiophene)

Poly(calix[4]arene bis-bithiophene) (poly(CalixBBT)), employs hinge molecules (calix[4]arene) interconnected by rigid rods (quarterthiophene). The rods attract one another in the oxidized state, contracting the material into a folded molecular structure. This molecular contraction is driven by the π–π dimerization (π–π stacking) of thiophene oligomers rods upon oxidation, producing a reversible molecular displacement [66]. The cone conformation of the calix[4]arene scaffold allows generation of an accordion-like molecule upon polymerization under either electrochemical or chemical conditions.

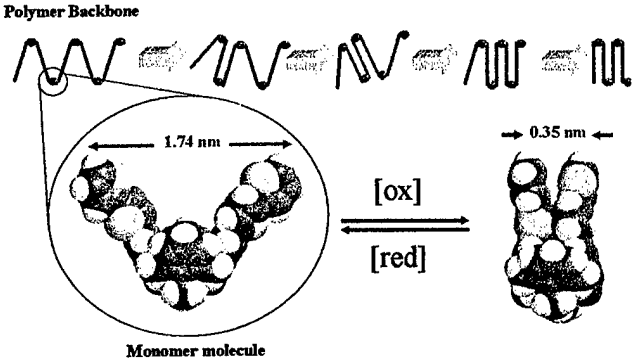

Figure1: Schematic of the actuation mechanism of poly(CalixBBT) [70].

Poly(calixBBT) is a promising actuating material. Key features of this material include the deformable calix[4]arene scaffold and the redox active quarterthiophene redox units. The proposed actuation mechanism and a 3-dimensional space-filling model are shown conceptually in Figure 1. The initial polymer displays an equilibrium conformation that has the quarterthiophene groups in a non-aggregated state. Upon oxidation the quarterthiophene groups have a strong tendency to aggregate into a π-stacked structure. Simple inspection of the space-filling model in suggests that one dimensional changes as large of a factor of 9 are possible . for Poly(calixBBT) [71].

The proposed molecular actuation mechanism presented above and referred as π-dimerization or π–π stacking makes use of wavefunction overlap in π–conjugated polymers. The π-dimerization is attractive in the oxidized state (electron

deficient) and repulsive in the reduced state (filled electronic levels) [66, 68-70].

It is hoped that these materials will overcome two important deficiencies of conducting polymer actuators, namely the limited strain and the low degree electromechanical coupling, while maintaining the advantage of low voltage operation. To date ~ 20 % strains have been observed in electrochemically activated π-π stacking polymers and tensile strengths are in the 10's of megapascals [65].

Limitations. This technology is in an early phase of research. A potential challenge is that the new molecules are unlikely to achieve the same high conductivity as polypyrrole and polyaniline. Low conductivity slows charging and reduces power output. However, conductivity is not as important in these new materials because the number of charges required to achieve displacement is substantially smaller (~100×).

G. *Carbon Nanotube Actuators*

TABLE VI
CARBON NANOTUBE ACTUATORS [72,73]

PROPERTY	MIN	TYP.	MAX	LIMIT
Strain (%)		0.2	1	1
Stress (MPa)		1		20,000
Work Density (kJ/m^3)		2		10^5
Strain Rate (%/s)		0.6	19	190,000
Power (W/kg)		10	270	10^{11}
Life (cycles)				
Coupling		0.00067		1.0
Efficiency (%)		0.1	18	100
Density (kg/m^3)		230	1000	2000
Modulus (GPa)	0.2	0.9	30	640
Tensile Strength (MPa)		5		40,000
Applied Potential (V)		1	30	4
Charge Transfer (C/m^3)		$6{\cdot}10^6$		$3{\cdot}10^7$
Conductivity (S/m)		40,000		500,000
Cost (US$/kg)		100,000		10

Mechanisms: Carbon nanotubes (CNT) are hollow cylinders consisting solely of carbon. These tubes have diameters that are typically 1.2 nm or larger. Their structure is that of a single rolled sheet of graphite. These sheets are either conductive or semi-conductive. CNT papers and fibers are filtered or spun from large numbers of nanotubes suspended in solution and are actuated by placing them in an electrolyte and activating them using an apparatus very similar to that used for conducing polymers. The application of potential causes the formation of an electrical double layer at the nanotube/electrolyte interface, in which the electronic charge stored in the carbon atoms is balanced by the ionic charge in the liquid phase. The accumulated charge stored in the nanotube is believed to cause a change in the C-C bond length during electron injection [72], producing strains of up to 1 %. Although the strains are small, individual carbon nanotubes are believed to exhibit tensile strengths exceeding 1 GPa, creating an unmatched work per actuator stroke.

As in conducting polymers, it is the rate at which charge can be injected which determines the strain rate. The enormous internal surface area provided by the carbon nanotubes results in an enormous capacitance (26 F/g) [73]. Given the applied potentials are on the order of 1 V, the resulting charge transfer is ~ 26 C/g. Once again the reduction of cell internal resistance is key to achieving high strain rates [46]. Rates of ion transport within the carbon nanotube papers and fibres may also limit rate, although this effect is smaller than in conducting polymers.

Materials & Dimensions: Carbon nanotubes can be synthesized by laser ablation, arc discharge, chemical vapour deposition and deposition from low cost precursors. They are commercially available from many sources. Typical sample dimensions are 30 μm thick, 10 mm wide and 30 mm long films [72,73].

Limitations: The small to moderate strains require some mechanical amplification for most applications. The electromechanical coupling is poor, requiring substantial energy recovery to achieve reasonable efficiencies. The material cost is currently very high (~$100/g). Films and fibres still exhibit bulk mechanical properties that fall far short of those of single nanotubes. This actuator technology is very new however, and progress on many of these issues is expected to be rapid.

Potential: Individual carbon nanotubes feature very large tensile strengths (>10 GPa) and moduli (640 GPa). If these properties can be approached in bulk materials, then the work density per cycle produced will be unmatched (~200 MPa). Use of thin films or fibers and closely spaced electrodes should also enable very high strain rates and power to mass ratios to be achieved [46], outperforming piezoceramic materials. Newly reported porous metals and oxides appear to be actuated using mechanisms similar to those in CNTs, and could provide high performance relatively soon at lower cost [74].

H. Ionic Polymer/Metal Composites (IPMC)

Overview: An ionic polymer-metal composite (IMPC) consists of a polymeric electrolyte sandwiched between two thin metal layers. Deflection of the layered structure towards one of the metal electrodes occurs as a result of a field induced change in ion concentration, which attracts water molecules to one side of the polymer. The non-uniform distribution of water produces swelling of one side of the actuator and contraction of the other. Unlike other actuator technologies that have been discussed, this technology does not produce significant linear actuation but only bending.

TABLE VII
IONIC POLYMER METAL COMPOSITES [75-80]

PROPERTY	MIN.	TYP.	MAX.
Strain (%)			3.3
Stress (MPa)			0.93
Work Density (kJ/m^3)			3

Strain Rate (%/s)			3.3
Power (W/kg)			8.23E-04
Coupling (%)			3
Efficiency (%)			3
Modulus (GPa)	0.1		1.8
Density (kg/m3)		2100	
Applied Potential (V)	2		7
Charge Transfer (C/m^3)		900,000	
Charge Transfer (C/m^2)		900	
Cost (US$/kg)	500	50000	

Mechanisms: When an electric field is applied across a strip of IPMC, the ions redistribute themselves, resulting in the formation of two thin boundary layers- a cation-poor layer on the anode side of the polymer and a cation-rich layer on the cathode side. As cations travel to the cathode side of the IMPC, water diffuses into the cation-rich clusters to neutralize the charge, causing the hydrophilic clusters to expand. The strain in the cathode layer induces stresses in the rest of the polymer matrix, resulting in a fast bending motion towards the anode [77,78]. After this immediate response, the pressure from the strained polymer matrix causes water to diffuse out of the cation-rich clusters, causing a slow relaxation towards the cathode [77,78]. Reversing the applied potential inverts the bending (and the relaxation). The degree of actuation exhibited is dependent on the type of polymer, the counter ion used, and amount of water present [77] as well as the quality of metallization [80], and thickness [75] and surface area of the polymer membrane [82].

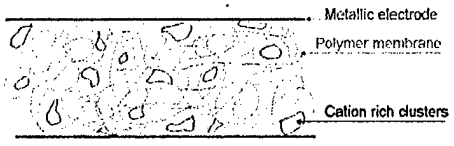

Neutral State: IMPC is flat

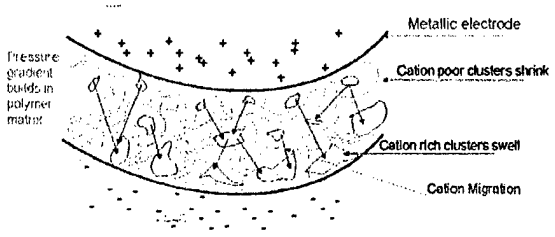

Applied potential causes cations migrate to cathode: IMPC contracts

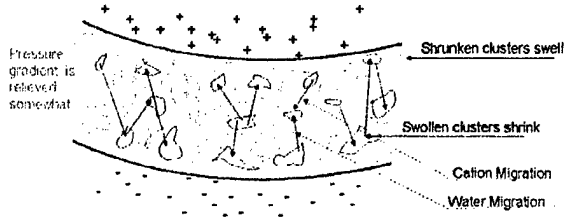

Pressure gradient causes water to flow towards anode: IMPC relaxes

Figure 2: IPMC Actuation.

Materials & Fabrication: Typical polymers are perfluorinated alkenes with anionic-group-terminated side chains, such as Nafion™ [75-76] and Flemion,™ [77] or styrene/divinylbenzene-based polymers with ionic groups substituted from phenyl rings [75-76]. Styrene/divinylbenzene based polymers tend to be highly cross-linked, so their potential as an actuator is severely limited by their stiffness. The perfluorinated alkenes form a more flexible matrix [75-76]. In any IMPC matrix, the backbone of the polymer is hydrophobic while the anions used to dope the polymer are hydrophilic. This causes the polymers to make clusters of concentrated anions, neutralizing cations and water within the polymer network [76-80].

In most cases, a commercially available polymer membrane is used for the polymer layer. These membranes are not manufactured specifically for IMPCs, however, and limit the IMPCs to a thickness of approximately 200μm [75]. Kim and Shahinpoor have addressed this problem by solution recasting Nafion™ film to a thickness ranging from 30μm to 2mm [75]. Noh et al. also used a recasting method to make Nafion™ membranes with much higher surface area [81].

Both sides of the polymer membrane are loaded with metal nanoparticles and then metal plated [75-80]. The nanoparticles balance the charging that occurs in the clusters in the boundary layers of the polymer, while the metal plating increases surface conductivity. The metal nanoparticles are usually 3-10 μm in diameter and are distributed in a 10 to 20 μm deep layer both surfaces. This is often done by allowing the polymer to soak in a solution containing a metal salt, such as $Pt(NH_3)_4HCl$, so the metal ions can diffuse into the polymer. The polymer is then treated with a reducing agent, such as $LiBH_4$ or $NaBH_4$, to metalize. The primary reaction for platinum IMPCs is as follows [75,90]:

$$LiBH_4 + 4[Pt(NH_3)_4]^{2+} + 8OH^- \Rightarrow 4Pt^o + 16NH_3 + LiBO_2 + 6H_2O \quad (2)$$

This metallization process is quite expensive, but Shahinpoor and Kim have shown one can reduce the cost by physically loading the metal particles into the polymer [76]. The polymer and metal powder can be composited by pressing under high pressure and temperature (Shahinpoor and Kim pressed under 2 tons at 130°C for 15 minutes, 3 times). The electrode layer can then be deposited onto the surfaces. IMPCs manufactured in this way have shown comparable properties to chemically loaded IMPCs, at 1/10 of the manufacturing cost [76].

After the metal particles have been incorporated into the polymer, a metal plating (usually 1 to 5 μm thick) is deposited [76]. This plating also involves reduction of a metal salt, but instead of impregnating the metal into the polymer the reaction coats the surface of the composite. Metals that have been successfully used for this process include platinum, palladium, silver, gold, carbon, graphite, carbon nanotubes [76,80] as well as copper 80]. Platinum is the most commonly used as it is has the widest potential region over which it is resistant to corrosion. The higher potential enables larger deflection and higher work density.

The electrode reduces the surface-electrode resistance down to as little as 8.6% of its original value [80].

IPMCs are further described in an article by Kim et. al. in this issue. Samples are now commercially available [82].

I. Magnetostrictives

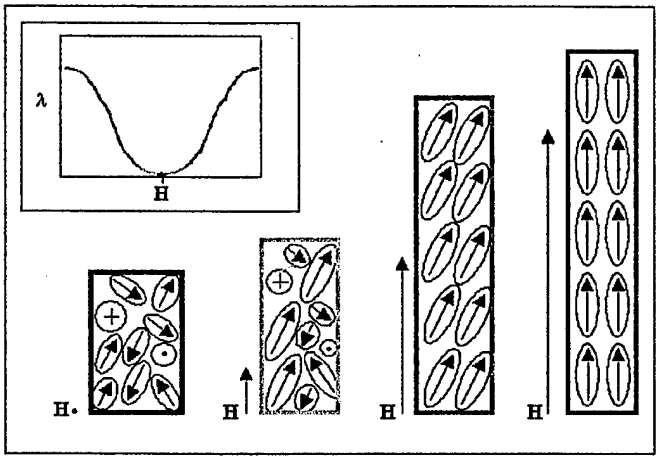

Figure 3: Magneto-striction.

History: Over a century after Joule's discovery of the conversion of magnetic energy to mechanical energy, the magnetostrictive effect again sparked scientific interest upon the discovery of giant magnetostriction in Lanthanide metals. Arthur Clark, in his early review of the subject [83], presents a detailed account of the investigations and insight that prompted the development of rare earth alloys capable of strains on the order of 1.0 x 10^{-3} at room temperature. This represented an increase of two orders of magnitude over magnetostrictive strains observed by Joule and obtainable in common transition metals such as Fe, Co, and Ni. By 1974, it was postulated that the alloy $Tb_{0.3}Dy_{0.7}Fe_2$ would exhibit large magnetostriction with a relatively small applied field at room temperature [84]. Indeed, nearly thirty years later, a commercially available product of the same nominal composition, known as Terfenol-D, is capable of producing strains of 1.6 x 10^{-3} with an applied field of 2.0 MA/m and power densities of 10-20 kJ/m^3 [85].

Mechanism: The process of magnetostriction makes use of the magnetic domains that form within a ferromagnetic material when cooled below its Curie Temperature (*Tc*). The presence of an external magnetic field first grows the domains aligned with the field and then overcomes the anisotropic energy to rotate the magnetic moments of the unaligned domains to a more favorable, easy axis in the crystal. The growth and rotations are accompanied by strains in the bulk material. Strengthening the field further aligns all of the domains completely with the field and leads to saturation. A schematic diagram of the magnetostrictive mechanism is presented in Figure 3 with a representative curve for strain versus applied magnetic field and coinciding with descriptions in the literature [84,85]. The performance of a magnetostrictive material can be well characterized by Curie Temperature *Tc*, saturation magnetostriction λs, and magnetic anisotropy energy *K*. Indeed it was an understanding of these properties that led to the development of Terfenol D [83] which combines a Tc of 380 °C, a λs of 1.6 x 10^{-3} and a K near zero. $TbFe_2$ and $DyFe_2$ have K values of opposite signs, making the minimization possible through variations in composition. Further work has demonstrated that magnetostrictive materials can be tailored for specific temperature regimes guided by the same principles [85].

Features: For room temperature applications, Terfenol-D is the highest performing magnetostrictive material. It is most commonly utilized in cylindrical forms and driven with solenoids. It has a modulus of 25-30 GPa with tensile and compressive strengths of 28 and 700 MPa respectively [87]. The material properties continue to be improved through numerous methods including single crystal growth, defect study and elimination, and crystal orientation [88], leading to strains of 2.4 x 10^{-3} [89]. Meanwhile, engineering applications have improved the performance of Terfenol-D by applying a bias field with permanent magnets to enable controlled positive and negative deflection and applying a prestress to the material, enabling larger strains by compressing the magnetic domains before the application of a magnetic field. In addition, careful use of device resonance has enabled the observations of dynamic strains of 3.5 x10^{-3} and approximately 50% of electrical energy being converted to work [92]. Cycle lives in the tens of millions have been suggested [87].

TABLE VIII
MAGNETOSTRICTIVE MATERIALS [WWW.EXTREMA.COM, 85]

PROPERTY	MIN.	TYP.	MAX.
Strain (%)		0.1	0.24
Stress (MPa)		20	28
Work Density (kJ/m^3)		20	
Strain Rate (%/s)		20 @10 kHz	
Life (cycles)			10^7
Coupling		0.75	
Density (kg/m^3)		9210	
Modulus (GPa)	25		35
Tensile Strength (MPa)		28	
Compressive Strength		700	
Applied field (MA/m)		2	

Limitations: The relatively small strains (0.1 to 0.25 %) observed in these materials mean that substantial mechanical amplification is required for many applications. These materials are brittle in tension, failing at stresses of 28 MPa. Magnetostrictive composites have enabled reductions in brittleness while maintaining large strains and increasing bandwidth [93]. Terfenol-D can operate in the frequency range of kHz, though its high conductivity leads to significant eddy currents at higher frequencies. Commercially, laminations of multiple crystals are used to minimize the eddy currents and extend the frequency range. Costs of Terfenol-D depend largely on the availability of the rare earth metals, though costs of high performance composites and single crystals are not yet available.

Temperature: All magnetostrictive materials reversibly lose functionality above *Tc*, while temperatures above the melting

point require reprocessing. There are no known material failure mechanisms comparable to depoling of piezoelectric transducers.

Modeling: In his first review, Clark discussed the effects of the magnetic field on the crystallographic planes of cubic and hexagonal lattices, which led to an abundance of characterization constants [83]. Since then, some authors have sought simplified device specific models [92], while others have developed theories based on free energy minimization [87]. Recently, Jiles has focused on the hysteretic effects of magnetoelasticity, a source of considerable difficulty in modeling for practical applications [86]. In his earlier review, however, Jiles gives an excellent description of the development of key parameters to be used in successful application of Terfenol-D [90]. While modeling represents the newest challenge for magnetostrictive materials, it's success has led to many innovations in materials and processing.

J. Thermally Activated Shape Memory Alloys (SMA)

History: Over a century after Joule's discovery of the equivalence of energy and heat the shape memory effect was reported by Chang and Read [96]. They observed that an alloy of gold and copper returns to the same shape if heated after deformation. The same effect was later discovered in Indium-Titanium alloys by Basinski and Christian [92], and Nickel-Titanium alloys by Buehler, Gilfrich and Wiley [95]. These researchers used the term "Shape Memory Effect" (SMA) to describe the phenomena. Of all the SMAs, Nickel Titanium (NiTi) alloys (better known as Nitinol) are the most extensively studied [98]. NiTi fibers and springs have often been studied and used as artificial muscles [94,99,101,103-105] because of their relative nontoxicity, reasonable cost and an electrical resistivity that easily lends itself to Joule heating (passing of an electrical current to generate heat).

TABLE IX
THERMAL SHAPE MEMORY ALLOYS [2]

PROPERTY	MIN.	TYP.	MAX.
Strain (%)		5	8
Stress (MPa)			200
Work Density (kJ/m^3)		>1000	
Strain Rate (%/s)		300	
Power (W/kg)		1000	>50,000
Life (cycles)	10	10000	10^7
Efficiency (%)		3	5
Modulus (GPa)	20		83
Tensile Strength (MPa)		1000	
Density (kg/m^3)		6450	
Applied Potential (V)	4		1 kV/m
Conductivity (S/m)		1250	1425
Cost (US$/kg)		300	

Mechanism: Martensitic transformations are at the heart of the shape memory effect as shown by Otsuka and Shimizu [107]. Martensitic transformations were discovered by the metallurgist Adolf Martens in steels [108]. It was found that the transformation from the high-temperature, body-centered cubic lattice austenitic phase to the low temperature, face-centered tetragonal lattice takes place without atomic diffusion. Martensitic transformations are phase changes that occur as a displacitive, lattice-distortive, first order diffusionless athermal transformations. In NiTi alloys with a surplus of nickel or with nickel partly replaced with a third element, a two stage martensitic transformation may occur. The intermediate phase has a rhombohedral crystal structure.

In most NiTi alloys the shape memory effect is only observed when an external stress is applied. In the martensitic phase the alloy has a twinned martensite that can be easily deformed as it de-twins. As it is heated it returns to its parent austenitic phase, which is a highly ordered state, and the alloys retrieves a well defined high-temperature shape.

NiTi alloys may also exhibit a two-way shape memory effect (TWSM) first observed by Delaey et al. in 1975 and by which the alloy will exhibit the shape memory effect without an external stress [97]. In the two-way shape memory effect NiTi alloys also have a "remembered" state at low temperature as well as all the intermediate shapes between the high temperature and low temperature. The origin of TWSM is stress-biased martensite and it can only be obtained by special conditioning involving thermo-mechanical treatment.

The contraction time of NiTi is governed by the speed at which the martensitic to austenitic phase transformation occurs and hence by the electrical power when electrical Joule heating is used. By using very large current pulses this contraction time can be reduced to several milliseconds [104]. The NiTi contraction and expansion cycles are mainly limited by the long time required for NiTi to cool and return to its lower temperature shape. The cooling time is governed by thermal diffusion and convection. Factors such as heat capacity and latent heat involved in the phase transformation between the austenitic and martensitic phases must be considered when designing an actuator.

Features: Shape memory alloys can exert very large forces per unit area (exceeding 200 MPa), operate at very high strain rates (300%/s) and undergo relatively large deformations (> 5% for poly-crystalline NiTi fibers). The peak energy density (10^7 J·m^{-3}) and power per unit mass (50 kW·kg^{-1}) of these actuators is unmatched.

Limitations: SMAs have several characteristics that impede their use as muscle-like actuators. One of them is the difficulty of controlling the length of NiTi fibers as they undergo a phase transformation. The change in length is observed over a narrow temperature range and a significant hysteresis is observed between the martensitic to austenitic and austenitic to martensitic phases. The phase transformation temperatures vary more or less linearly with stress and the cycling characteristics also change if only partial transformations occur. All of these factors must be modeled appropriately when NiTi fibers are used in a servo-actuator.

NiTi actuators also have a limited lifetime in terms of useable cycles. At very large strains their shape memory effect degrades significantly, from millions of cycles at 0.5%

strains to a few hundred cycles at strains of 5% [98] depending on the alloy and conditioning. Their usage is also limited by the low efficiency of NiTi fibers in converting electrical energy to mechanical work which is typically found to be limited to less than 5% (including recovery of energy from heat, [106]).

Materials: Nickel titanium shape memory alloys are commercially available from several sources including Shape Memory Applications Inc. http://www.sma-inc.com/.

Applications: NiTi wires, tubes and components are widely used in medical applications due to their super-elasticity, a property related to the memory effect. Little use is made of the actuation properties.

K. Ferromagnetic Shape Memory Alloys (FSMA)

Overview: FSMAs utilize crystallographic transformations to macroscopically change dimension under the influence of a magnetic field. Following the discovery of the thermally induced martensitic transformation in the ferromagnetic Ni_2MnGa Heusler alloy in 1995 [111], it was postulated that large strains could also be obtained magnetically. Scarcely a year later, strains of 0.2% were observed in a single crystal of the same composition upon the rotation of a magnetic (H) field of order 600 kA/m [112]. Further investigation into the effects of varying the atomic composition of the alloy on the martensitic transition and Curie temperatures [113] along with better characterization techniques have since led to measurements of 6% [114] and even 10% [115] linear strain under applied fields of the same order of magnitude. These strains may be obtained against stresses of order 1 MPa and with response times in milliseconds at room temperature.

TABLE X
FERROMAGNETIC SHAPE MEMORY ALLOYS [113-11,118]

PROPERTY	MIN.	TYP.	MAX.
Strain (%)			10
Stress (MPa)	0.005	1	9
Work Density (kJ/m^3)		95 2000	
Strain Rate (%/s)		(10% @ 100Hz)	
Coupling (%)		75	
Cost (US$/kg)		4400	

Mechanism:
The mechanism encompasses transitions from the cubic austenite phase to the tetragonal martensite phase as well as transitions between variants of the martensite phase. The martensite phase is magnetically easy along its shortest (c) axis and may be aligned mechanically or magnetically. Typically, samples are prestressed in compression to align the anisotropic unit cells. Upon the application of a magnetic field orthogonal to the direction of stress, regions of the magnetically favored variant nucleate and grow. These regions may be monitored by the appearance of twin boundaries, which are observed to move along the sample as the intensity of the field is increased [116,117]. The magnitude of the bias or prestress is important as an insufficient stress will leave the sample uncompressed and an overstress will block the transition. Blocking stresses between 2.0 and 9 MPa have been reported [114,118]. Following the removal of the field, stresses above 0.5 MPa are sufficient to return the sample to original dimensions [114].

Modeling: O'Handley et. al. recently reviewed the models currently used in predicting strain vs. magnetic field for FSMAs [119].

Materials: Single crystal Ni_2MnGa and slight variations are used. Other ferromagnetic alloys (such as Fe-Pd and Fe-Ni-Co-Ti) show similar effect, but lower strains. Polycrystalline Ni_2MnGa also exhibits FSMA behavior, but at reduced strains due to alignment and loading within a matrix [120].

Features: Large strains (~10%) are obtained for a stiff (up to 90 GPa modulus) crystalline alloy system. Fast response (~ 1kHz) and high cycle life (~5×10^7 cycles) are also observed [121].

Limitations: High intensity magnetic fields are required (~500 kA/m) and the fields need to be applied orthogonal to stroke direction, adding challenge to the device design. Although the stresses against which the actuators will work are relatively large (up to ~ 1 MPa), this stress value does not account for the cross-sectional area needed to generate the magnetic fields. For example, in Adaptamat Ltd. products the active material produces 1 MPa stresses, but once the coils necessary to produce field are added, the effective stress drops to < 20 kPa [121]. The presence of the coils also drops the work density to 0.12 kJ·m^{-3}. Furthermore, repeated actuation requires a compressive restoring force (e.g. a spring). Finally, modulus appears to change tremendously between the Austenite and Martensite phases (dropping to 0.02 GPa in the Martensite phase [123]). The compliance may result in low resonance frequencies.

Temperature: Operation must be near the martensitic transformation temperature (ranging between 200- 350 K) and below Curie temperature (325-350 K), both of which vary with composition [112].

Applications: Linear motors are available from Adaptamat Ltd. operating with strains ~3% at 2 MPa (not including the electromagnets).

Potential: Achieved strain has reached the known theoretical limit. However, new passive shape memory effect discoveries may lead to higher strains [122].

III. CASE STUDIES

Two case studies that represent promising applications of artificial muscle technology are presented. Both applications are targeted at autonomous underwater vehicles (AUV), where size, power consumption and cost need to be minimized. In the first case, varying propeller blade camber using artificial muscle is proposed. In the second, amplification of propeller thrust by the generation of unsteady flow is presented. In the first application rates are relatively slow – the challenge is to incorporate the actuator within the space allotted. In the second, power to mass and fuel efficiency become critical.

A. Case Study: Variable camber propeller

Controllable pitch propellers are employed in situations where vessels operate under a range of flow conditions. The complex gearing mechanisms employed are too costly to consider in most AUVs. Nevertheless AUVs could benefit tremendously from the added efficiency, maneuverability, and the potentially lower noise emissions afforded by variable shape propellers.

The target vehicle for variable camber is EMATT (Expendable, Mobile ASW Training Target from Sippecan Inc, in Marion, Massachusetts). The expendable nature of the vehicle makes cost a key consideration.

Specifications: This design is for a propeller blade that has a span (length) of 50 mm, a chord (width) of 25 mm, and an average thickness of 6 mm. The last 10 mm of the chord at the trailing edge are pivoted so as to have variable camber. Figure 4 shows the approximate geometry. The angle of the trailing edge is to be adjusted by 45° under a force load of up to 3.5 N.

In order to simplify the calculations the unknown distribution of the force is applied at a single point at 3 mm from the trailing edge. The force of 3.5 N generates a torque of 25 mN·m about the pivot. If the angle of deflection is 45°, the work that must be done is $W = T\,\theta = (25\text{ mN m})\times(\pi/4) =$ 19 mJ. A DC electrical power source capable of delivering up to 9 A at 45 V is available at the propeller. The vehicle lifetime is up to ten hours, over which time up to 10,000 actuation cycles will be performed.

Will the actuator fit within the space?

Ideally the mechanism employed will fit within a propeller blade. The non-pivoting portion of each blade has a volume of 6 mm × 15 mm × 50 mm = 4.5×10^{-6} m^3. Given the required work, the minimum work density in order to fit the actuator within the propeller volume is 4.2 kJ·m^{-3}. The higher the work density of an actuator material is above this value, the lower the volume that will be required and the easier will be the fit.

TABLE XI: COMPARISON OF WORK DENSITIES

MATERIAL	WORKDENSITY (KJ/M3)
Skeletal Muscle	0.8
FSMA including coils	<1
Dielectric Elastomer (Silicone)	1.6
Carbon Nanotubes	2
IPMC	3
Magnetostrictive	20
Liquid Crystal Elastomer	56
Dielectric Elastomer (VHB)	58
Ferromagnetic SMA	95
Conducting Polymer	100
Ferroelectric Polymers	320
Thermal SMA	1000

The data in Table XI suggest that skeletal muscle, silicone dielectric elastomers, carbon nanotubes and IPMCs do not currently demonstrate sufficient work density for this application. Inclusion of activation coils needed to generate magnetic field in the energy density calculation eliminates the FSMA (and the magnetostrictives, which require still higher fields). Note that the lower energy densities of these technologies could be compensated for by using multiple actuator strokes to deflect the trailing edge (e.g. using a ratchet mechanism). However, this adds to the complexity and cost of the device.

Mechanical Amplification: The linear actuators discussed range in strain from less than 1% to more than 100%, and the stresses from the low kPa range up to 200 MPa. If the force divided by the cross-sectional area (3.5 N/(50 mm×6 mm)=12 kPa) is less than the stress that an actuator is capable of generating, then no amplification of the force is required. Furthermore, if the strain multiplied by the length of the actuator is roughly equal to the required displacement of the trailing edge (=3 mm×sin(45°)/15mm= 14 % strain), then little or no amplification of the strain is required, simplifying design and fabrication. The ideal actuator will feature both high strain and high stress. Low values of either indicate a need for mechanical amplification, and the smaller the values the greater the amplification. For example, the small strains characteristic of magnetostrictive materials need to be amplified by a factor of ~100. This degree of amplification is unrealistic without resorting to a stepping or ratcheting motion.

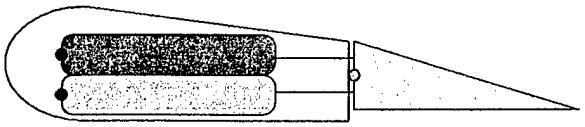

Figure 4: Lever arm design for creating variable camber.

Example – LCE Acutation

To make these considerations more concrete, consider designing an LCE actuator for this application. The best performance of a thermal liquid crystal elastomer reported in the literature [38] has a work density of $\sigma\times\varepsilon$ = (140 kPa)×(0.40) = 56 J/m^3, well over the required work density.

As a simple design exercise, we can model a lever arm that pulls around the pivot. If the muscle attachment points are a distance of 1 mm from the pivot (in the vertical direction), the muscles must exert a force F to balance the torques:

$$F = \frac{(3.5N)(7mm)}{(2mm)} = 12.5N. \quad (4)$$

The liquid crystal elastomer can exert a stress of 140 kPa and undergo a strain of up to 40%. The cross-sectional area needed to generate a force of 12.5 N is:

$$A = \frac{12.5N}{140kPa} = 90 \times 10^{-6} m^2, \quad (5)$$

or, if the width of the muscle is taken to be the length of the blade (50 mm), the thickness h of the muscle must be:

$$h = \frac{A}{L} = 1.8mm \quad (6)$$

The muscle length that is needed to get a 45° rotation of the trailing edge is roughly $\Delta x = 2\ mm \times \sin(45°) = 1.4\ mm$. If the total strain of the actuator is 40%, then an actuator length of only 3.5 *mm* is needed to give the required deflection. The calculations show that an LCE actuator could be used for this application based on these considerations alone.

Rate: In changing camber, a 1 s response time is ample. All the actuators presented can reach this target. However, in conducting polymers the actuator material thickness cannot exceed ~ 30 μm if the actuator is to respond within 1 s – otherwise diffusion of ions into the polymer will be too slow. A laminated or porous structure is required. Thermally activated liquid crystal elastomers, in which heat must be transferred to or from the polymer, will also need to be laminated into similarly thick layers, and have a mechanism for transferring heat to each layer.

Voltage Requirements: Ferroelectric polymers, dielectric elastomers and, to a lesser degree, liquid crystal elastomers all require high fields in order to produce substantial displacement. In order to prevent voltages from being excessive, these materials will need to be layered. 100 μm thick layers require 1.5 kV in ferroelectric polymers and dielectric elastomers, and as low as 150 V in liquid crystal elastomers (LCE). For optimum performance, these layers should also be pre-strained, adding to complexity of assembly. Note that for the ferroelectrics and dielectric elastomers in particular, additional cost and space will be needed for DC-DC power converters.

Catch state: In varying camber it is anticipated that one angle of deflection may prove optimal over long periods of time. Thus it best if no power input is required to maintain the desired position. Thermally activated SMAs and LCEs generally require continued heat input in order to hold a fixed position, and thus consume substantial power even when no work is being performed. IPMCs are often characterized by substantial leakage current to maintain fixed position, and in some cases cannot hold a position for more than several seconds. As a result, SMAs and LCEs are not suited for steady state applications.

Continuously variable positioning: SMAs and LCEs involve phase changes. It is easy to run these phase changes to completion each time actuation is performed, but it is a challenge to control the phases such that an intermediate state is reliably reached. For this reason SMAs and LCEs are not appropriate for the variable camber application.

Having considered energy density, mechanical amplification, voltage, controllability, and energy expenditure, each actuator technology may be accepted or rejected, as presented in Table XII.

TABLE XII
ACTUATOR SELECTION: VARIABLE CAMBER

MATERIAL	ACCEPT?	POTENTIAL PROBLEMS
Skeletal Muscle	No	Work density too low.
Ferromagnetic SMA	No	Coil volume prohibitive.
Dielectric Elastomer (Silicone)	No	Work density too low.
Carbon Nanotubes	No	Work density too low.
IPMC	No	Work density too low.
Magnetostrictive	No	Coil volume prohibitive.
Liquid Crystal Elastomer	o.k.	Control & lamination?
Dielectric Elastomer (VHB)	o.k.	Stiffness & high voltage.
Conducting Polymer	o.k.	Lamination.
Ferroelectric Polymers	o.k.	High voltage.
Thermal SMA	No	Control, no catch state.

There are four candidate actuator technologies that are likely suitable for the variable camber application.

B. *Case Study 2: Unsteady Flow Hydrodynamics*

The work of MacLetchie et. al. [124] demonstrates that adding flapping and rolling motions in a critical range of frequencies to foils and propellers can quadruple thrust for a given propeller rotation rate. Can the artificial muscle technologies meet the demands of this high power application?

The REMUS AUV (http://www.hydroidinc.com/) is chosen as an example platform for application of novel propulsion concepts. REMUS has been selected by the Navy for performing Very Shallow Water Mine Counter Measures (VSW-MCM).

Rate: The REMUS propeller runs at ~ 25 Hz. To create optimum unsteady flow conditions, the blades must then flap at ~ 50 Hz. This bandwidth requirement immediately eliminates thermally activated LCEs, and conducting polymers as candidate materials. As discussed above, it should be possible to drive these materials up to kilohertz frequencies, but current demonstrations operate at only 1Hz.

Cycle Life: A REMUS mission lasts up to 22 hours, which corresponds to ~ 2 million actuator cycles. This cycle number is approaching or exceeding the limits so far measured for most technologies. In order to achieve this cycle number, the amplitude of actuation will need to be reduced to < 3 % in thermally activated SMAs. Actuators will generally need to be replaced following each mission.

Input Energy & Power: REMUS is equipped with a 1 kW·hr Lithium Ion cell. Thermally activated SMAs and LCEs as well as conducting polymers and IPMCs all operate at low voltages and with high currents. The low electromechanical coupling of these actuators results in input electrical powers

that are ~ 100 × greater than the work output. Although voltages are similar to those used in electromagnetic drive motors, the currents are ~ 100 × larger. The battery drains 100 × faster, and 100 × more power is demanded. Effectively, the battery mass must be increased by two orders of magnitude, and thus these actuator technologies are not practical for this high bandwidth, finite energy supply application.

In ferroelectrics and dielectric elastomers in particular DC-DCs converter will be required. It remains to be determined how much space this will occupy over and above the cell. Energy recovery circuitry may also be required to obtain reasonable efficiencies and mission lengths in these actuators, as well as in magnetostrictive materials.

Results: Based on preliminary design considerations, ferroelectric polymers and possibly dielectric elastomers are the most promsing technologies for generating unsteady flow in REMUS, providing the necessary high voltages can be generated.

IV. Discussion

Table XIII presents a summary of the properties of the actuator technologies discussed.

TABLE XIII
ACTUATOR SUMMARY

Actuator	Advantages	Disadvantages	Comments
Mammalian Skeletal Muscle	Large strains (20 %). Moderate Stress (350 kPa peak). Variable stiffness. High energy density fuel (20-40 MJ/kg). Efficient (~ 35 %). Moderate work density (0.8 kJ/kg). High cycle life (by regeneration).	Not yet an engineering material. Narrow temperature range. No catch state (expends energy to maintain a force w/o moving, unlike mollusk muscle)	Incredibly elegant mechanism that is a challenge to emulate. Muscle is a 3D nanofabricated system with integrated sensors, energy delivery, waste/heat removal, local energy supplies and repair mechanisms.
Dielectric Elastomers	Large strain (20%-200 %). Moderate stress (several MPa peak). Large work density (up to 58 kJ/m^3) Moderate to high bandwidth (7 Hz to > 1 kHz depending on the material and the geometry). Low cost. Low current. Good electromechanical coupling (>6%) and efficiency (potentially 60% with energy recovery circuitry).	High voltages (> 1 kV) and fields (~150 MV/m),. Typically requires DC-DC converters. Compliant (E < 1 MPa) & creeps. Pre-stretching mechanisms currently add substantial mass and volume, reducing actual work density and stress.	Potential to lower fields using high dielectric materials. Small devices are favored for high frequency operation (due to the more efficient heat transfer which prevents thermal degradation, and higher resonant frequencies). Starting materials are readily available.
Ferroelectric Polymers	Moderate strain (< 5 %). High stress (< 45 MPa). Very high work density (up to 1 MJ/m^3). Stiff (~0.4 GPa). High bandwidth (> 100 kHz in small devices). Strong coupling (45%) & efficiency. Low current.	High voltages (typically > 1kV) and fields (~150 MV/m). Typically need DC-DC converters. Synthesis of typical materials involves environmentally regulated substances. Cycle life is unclear & may be limited by electrode fatigue.	Lower voltages and fields are being achieved using new high dielectric composites. Small devices are favored for high frequency operation eg. MEMS.
Liquid Crystal Elastomers	Large strains in thermally induced materials (45%). Moderate strains in field induced materials (2-4 %). High coupling (75%) in electrical materials.	Subject to creep. Thermal versions are slow unless very thin or photoactivated Relatively high fields (1-25 MV/m). Low efficiency in thermal materials.	New material with much promise and much characterization to be done.
Conducting Polymers	High stress (34 MPa max, 5 MPa typ.). Moderate strain (2 %). Low voltage (2 V). High work density (100 kJ/m^3). Stiff polymer (~ 1 GPa).	Low electromechanical coupling. Currently slow (several hertz maximum to obtain full strain). Typically needs encapsulation.	Promising for low voltage applications. Speed and power will improve dramatically at small scales.
Molecular Actuators	Large strain (20 %). Moderate to high stress (> 1 MPa). Low voltage (2 V). High work density (> 100 kJ/m^3)	Currently slow. Needs encapsulation.	Great promise of overcoming many of the shortcomings of conducting polymer actuators, but still very early in development.
Carbon Nanotubes	High stress (> 1 MPa). Low voltage (2 V).	Small strain (0.2 % typical). Currently has low coupling. Needs encapsulation. Materials are presently expensive.	Great potential as bulk materials approach properties of individual nanotubes.
Ionic Polymer Metal Composites (IPMC)	Low Voltage (< 10 V). Large displacement (mechanical amplification built into the structure).	Low coupling and efficiency. Usually no catch state (consumes energy in holding a position). Requires encapsulation.	IPMC driven toys now available.
Giant Magnetostrictive Materials	High stress (<28 MPa). High work density (20 kJ/m^3). High frequency (> 10 kHz).	Large magnetic fields required which reduce the effective work and power to mass. Strains are small (0.2 %)	Readily available.
Thermally Activated Shape Memory Alloys	Very high stress (200 MPa). Unmatched power to mass (> 100 kW/kg). Moderate to large strain (1-8 %). Low voltage (actual voltage depends on wiring). Great work density (> 1 MJ/m^3)	Difficult to control (usually run between fully contracted and fully extended but not between). Large currents and low efficiencies (<5%). Cycle life is very short at large strain amplitudes.	Readily available.
Ferromagnetic Shape Memory Alloys	High stress (<9 MPa). High frequency (> 100 Hz). Moderate strain (up to 10%). High coupling (75%).	Bulky magnets required. Costly single crystal materials.	Operates in compression. Needs a restoring force.

REFERENCES

[1] J. Hollerbach, I. Hunter & J. Ballantyne "A comparative analysis of actuator technologies for robotics", O. Khatib, J. Craig & Lozano-Perez Eds, *The Robotics Review* 2, MIT Press, Cambridge MA 1992, pp. 299-342.

[2] I. Hunter & S. Lafontaine, "A comparison of muscle with artificial actuators", *Technical Digest IEEE Solid State Sensors & Actuators Workshop*, 1992, pp. 178-185.

[3] Y. Bar-Cohen ed. *Electro Active Polymers (EAP) as Artificial Muscles, Reality Potential and Challenges*, 67-83, SPIE Press 2001.

[4] Y. Bar-Cohen,2003 [Online]: Available http://ndeaa.jpl.nasa.gov/nasa-nde/lommas/eap/EAP-web.htm.

[5] M. Zupan, M.F. Ashby and N.A. Fleck, "Actuator classification and selection" *Advanced Engineering Materials*, vol. 4, pp. 993-940, 2002.

[6] R. Full and K. Meijer "Metrics of natural muscle." In *Electro Active Polymers (EAP) as Artificial Muscles, Reality Potential and Challenges*, ed. Y. Bar-Cohen, 67-83. SPIE Press 2001.

[7] W.C. Roentgen, "About the changes in shape and volume of dielectrics caused by electricity", Section III in G. Wiedemann Ed. *Annual Physics and Chemistry Series*, vol. 11, J.A. Barth, Leipzig, Germany pp. 771-786, 1880 (in German).

[8] R.Kornbluh, R.Pelrine, Q. Pei, S. Oh, J. Joseph, "Ultrahigh strain response of field-actuated elastomeric polymers" Smart Structure and Materials 2000, Electroactive Polymer Actuators and Devices, Proc. SPIE Vol. 3987 (2000), pp. 51-64.

[9] S. Ashley, "Artificial Muscles", *Scientific American*, pp. 52-59, October 2003.

[10] G.Kofod "Dielectric Elastomer Actuators" Ph.D. thesis, The Technical University of Denmark, September 2001

[11] P.Sommer-Larsen "Final report about ARTMUS-Artificial Muscles project" Riso National Laboratory, December 2001

[12] P.Sommer-Larsen, G.Kofod, S. MH, M. Benslimane, P. Gravesen, "Performance of dielectic elastomer actuators and materials" *Smart Structures and Materials, Electroactive Polymer Actuators and Devices*, Proc. SPIE Vol. 4695, pp. 158-166, 2002.

[13] R. Pelrine, R. Kornbluh, Q. Pei, S. Stanford, S. Oh, J. Eckerle, "Dielectric Elastomer Artificial Muscle Actuators: Toward Biomimetic Motion", *Smart Structures and Materials, Electroactive Polymer Actuators and Devices*, Proc. SPIE Vol. 4695, pp. 126-137, 2002.

[14] M. Benslimane, P. Gravesen, "Mechanical properties of Dielectric Elastomer Actuators with smart metallic compliant electrodes", *Smart Structure and Material, Electroactive Polymer Actuators and Devices*, Proc. SPIE Vol. 4695, pp. 150-157, 2002.

[15] G. Kofod, R. Kornbluh, R. Pelrine, P. Sommer-Larsen, "Actuation response of polyacrylate dielectric elastomers" *Smart Structure and Materials, Electroactive Polymer Actuators and Devices*, Proc. SPIE Vol. 4329, pp. 141-147, 2001.

[16] R. Pelrine, R. Kornbluh, G. Kofod, "High strain Actuator Materials Based on Dielectric Elastomers" *Advanced Materials*, Vol.12, Issue 16 1223-1225 Aug 2000.

[17] R. Pelrine, R. Kornbluh, J. Joseph, S. Chiba "Artificial Muscle for Small Robots" *Transactions of the Institute of Electrical Engineers of Japan* Vol. 122 No.2 pp.97-102, 2002.

[18] P.Sommer-Larsen, J. HookerG.Kofod, K. West, M. Benslimane, P. Gravesen, "Response of dielectric elastomer actuators" *Smart Structure and Materials, Electroactive Polymer Actuators and Devices*, Proc. SPIE Vol. 4329, pp. 157-163 2001.

[19] Q.M. Zhang, J. Li, M. Poh, F. Xia, Z.-Y. Cheng, H. Xu & C. Huang, "An all-organic composite actuator material with a high dielectric constant", *Nature*, vo. 419, pp. 284-287, 2002.

[20] Zhang, Qiming; Scheinbeim, Jerry, "Electric EAP" in *Electroactive Polymer Actuators as Artificial Muscle*, Y. Bar-Cohen, Ed. Bellingham, Washington: SPIE Press, 2001, pp.89-117.

[21] Zhang, Q. et al, "P(VDF-TrFE)-based Electrostrictive Co/Ter-Polymers and its Device Peformance" in *Electroactive Polymer Actuators and Devices*, Y. Bar-Cohen, Ed. Bellingham, Washington: SPIE Press, 2001, pp. 106-116.

[22] Bharti, V. et al, "High Dielectric Constant Composites Based on Metallophthalocyanine Oligomer and Poly(vinylidene fluoride-trifluoroethylene) Copolymer" in *Journal of Applied Polymer Science*, Wiley & Sons, Inc., Vol. 82, 70-75, 2001, Vol. 82, 70-75.

[23] Tashiro, K.; Nishimura, S.; Kobayashi, M., "Thermal Contraction and Ferroelectric Phase Transition in Vinylidene Fuoride-Trifluoroethylene Copolymers. 1. An Effect of Tensile Strength along the Chain Axis" in Macromolecules, ACS, 1988, Vol 21, 2463-2469.

[24] U.S. Patent # 6,355,749 (Outlines manufacturing. Also gives wide range of values for dielectric constants. Discusses dielectric constant temperature dependence and Curie temperature transition at room temp for terpolymer (a relaxor).

[25] Zhang, Q.M. et al, "Electrostrictive poly(vinylidene fluoride-trifluoroethylene) copolymers", Sensors and Actuators A,, Vol 90, 2001, 138-147.

[26] Zhang, Q.M, et al, "Poly(vinylidene fluoride-trifluoroethylene) Based High Performance Electroactive Polymers", in *Electroactive Polymer Actuators and Devices*, Y. Bar-Cohen, Ed. Bellingham, Washington: SPIE Press, 2003, pp. 133-142.

[27] Brand, H. R. Electromechanical Effects in Cholesteric and Chiral Smectic Liquid-Crystalline Elastomers. *Makromolekular Chemie-Rapid Communications*. 1989 Sep; 10(9):441-445.

[28] Finkelmann, H.; Nishikawa E.; Pereira G., and Warner M. A New Opto-Mechanical Effect in Solids. Physical Review Letters. 2001 Jul 2; 87(1).

[29] Kremer, F.; Skupin, H.; Lehmann, W.; Hartmann, L.; Stein, P., and Finkelmann, H. Structure, Mobility, and Piezoelectricity in Ferroelectric Liquid Crystalline Elastomers.; 113 pp. 183-201. (Advances in Chemical Physics.

[30] Lehmann, W.; Hartmann, L.; Kremer, F.; Stein, P.; Finkelmann, H.; Kruth, H., and Diele, S. Direct and Inverse Electromechanical Effect in Ferroelectric Liquid Crystalline Elastomers. Journal of Applied Physics. 1999 Aug 1; 86(3):1647-1652.

[31] Lehmann, W.; Leister, N.; Hartmann, L.; Geschke, D.; Kremer, F.; Stein, P., and Finkelmann, H. Piezoelectric and Pyroelectric Investigations on Microtomized Sections of Single-Crystalline Ferroelectric Liquid Crystalline Elastomers (Sc-Flce). *Molecular Crystals and Liquid Crystals Science and Technology Section a-Molecular Crystals and Liquid Crystals*. 1999; 328:437-445.

[32] Lehmann, W.; Skupin, H.; Tolksdorf, C.; Gebhard, E.; Zentel, R.; Kruger, P.; Losche, M., and Kremer, F. Giant Lateral Electrostriction in Ferroelectric Liquid- Crystalline Elastomers. *Nature*. 2001 Mar 22; 410(6827):447-450.

[33] Leister, N.; Lehmann, W.; Weber, U.; Geschke, D.; Kremer, F.; Stein, P., and Finkelmann, H. Measurement of the Pyroelectric Response and of the Thermal Diffusivity of Microtomized Sections of 'single Crystalline' Ferroelectric Liquid Crystalline Elastomers. Liquid Crystals. 2000 Feb; 27(2):289-297.

[34] Meier, W. and Finkelmann, H. Liquid-Crystal Elastomers With Piezoelectric Properties. Mrs Bulletin. 1991 Jan; 16(1):29-31.

[35] Roy, S. S.; Lehmann, W.; Gebhard, E.; Tolksdorf, C.; Zentel, R., and Kremer, F. Inverse Piezoelectric and Electrostrictive Response in Freely Suspended Flc Elastomer Film as Detected by Interferometric Measurements. Molecular Crystals and Liquid Crystals. 2002; 375:253-268.

[36] Shenoy, D. K.; Thomsen, D. L.; Srinivasan, A.; Keller, P., and Ratna, B. R. Carbon Coated Liquid Crystal Elastomer Film for Artificial Muscle Applications. *Sensors and Actuators a-Physical*. 2002 Feb 28; 96(2-3):184-188.

[37] Skupin, H.; Kremer, F.; Shilov, S. V.; Stein, P., and Finkelmann, H. Time-Resolved Ftir Spectroscopy on Structure and Mobility of Single Crystal Ferroelectric Liquid Crystalline Elastomers. Macromolecules. 1999 Jun 1; 32(11):3746-3752.

[38] Thomsen, D. L.; Keller, P.; Naciri, J.; Pink, R.; Jeon, H.; Shenoy, D., and Ratna, B. R. Liquid Crystal Elastomers With Mechanical Properties of a Muscle. Macromolecules. 2001 Aug 14; 34(17):5868-5875.

[39] Thomsen, D. L.; Keller, P.; Pink, R.; Naciri, J.; Shenoy, D., and Ratna, B. R. Mechanical Responses Approaching Stress, Strain, and Time Scale Properties of Muscle Using Anisotropic Liquid Crystalline Elastomers (Lces). Abstracts of Papers of the American Chemical Society. 2000 Aug 20; 220:272-PMSE.

[40] C.H. Huang, Q. Zhang and A. Jakli, "Nematic Anisotropic Liquid-Crystal Gels", *Advanced Functional Materials*, vol. 13, pp. 525-529, 2003.

[41] R. H. Baughman, Conducting polymer artificial muscles, *Synthetic Metals*, vol. 78, pp. 339-353, Apr 15, 1996.

[42] Pei, Q. and Inganas, O., Electrochemical Application of the bending beam method. 1. Mass transport and volume changes in polypyrrole

during redox. *Journal of Physical Chemistry*, vol. 96, pp. 10507-10514, 1992.

[43] Otero, T. F. Artificial Muscles, electrodissolutoin and redox processes in conducting polymers. In: *Handbook of organic and conductive molecules and polymers*, ed. Nalwa, H. S. Chichester: John Wiley & Sons, 1997.pp. 517-594.

[44] Herod, T. E. and Schlenoff, J. B., Doping induced strain in polyaniline: stretchoelectrochemistry *Chemistry of Materials*, vol. 5, pp. 951-955, 1993.

[45] Madden, J. D., Madden, P. G., Anquetil, P. A., and Hunter, I. W., Load and time dependence of displacement in a conducting polymer actuator *Materials Research Society Proceedings*, vol. 698, pp. 137-144, 2002.

[46] J. D. Madden, P. G. Madden, and I. W. Hunter, Conducting polymer actuators as engineering materials. In: *Proceeding of SPIE Smart Structures and Materials 2002: Electroactive Polymer Actuators and Devices*, ed. Yoseph Bar-Cohen. Bellingham, WA : SPIE Press, 2002.pp. pp. 176-190.

[47] Mazzoldi, A., Della Santa, A., and De Rossi, D. Conducting polymer actuators: Properties and modeling. In: *Polymer Sensors and Actuators*, eds. Osada, Y. and De Rossi, D. E. Heidelberg: Springer Verlag, 1999.

[48] Madden, J. D. Conducting Polymer Actuators. In: *Ph.D. Thesis*, Anonymous Cambridge, MA: Massachusetts Institute of Technology, 2000. available online from http://library.mit.edu.

[49] Madden, J. D., Madden, P. G., and Hunter, I. W. Characterization of polypyrrole actuators: modeling and performance. In: *Proceedings of SPIE 8th Annual Symposium on Smart Structures and Materials: Electroactive Polymer Actuators and Devices*, ed. Yoseph Bar-Cohen. Bellingham WA: SPIE, 2001.pp. 72-83.

[50] Kaneko, M., Fukui, M., Takashima, W., and Kaneto, K., Electrolyte and strain dependences of chemomechanical deformation of polyaniline film *Synthetic Metals*, vol. 84, pp. 795-796, 1997.

[51] Baughman, R. H., Shacklette, R. L., and Elsenbaumer, R. L. Micro electromechanical actuators based on conducting polymers. In: *Topics in Molecular Organization and Engineering, Vol.7: Molecular Electronics*, ed. Lazarev, P. I. Dordrecht: Kluwer, 1991.pp. 267

[52] Ding, J., Liu, L., Spinks, G. M., Zhou, D., Wallace, G. G., and Gillespie, J., High performance conducting polymer actuators utilizing a tubular geometry and helical wire interconnects *Synthetic Metals*, vol. pp. 8In Press.

[53] Kaneto, K., Kaneko, M., Min, Y., and MacDiarmid, A. G., "Artificial muscle" : Electromechanical actuators using polyaniline films *Synthetic Metals*, vol. 71, pp. 2211-2212, 1995.

[54] Yamaura, M., Hagiwara, T., and Iwata, K., Ehancement of electrical conductivity of polypyrrole film by stretching: counter ion effect *Synthetic Metals*, vol. 26, pp. 209-224, 1988.

[55] Wallace, G. , Zhou, D., Ding, J., Xi, B., Innis, P., Mazurkiewicz, J., Spinks, G., Gillespie, J., MacFarlane, D., Forsyth, S., and Forsyth, M., Ionic liquids and helical interconnects: bringing the electronic braille screen closer to reality *Proceedings of SPIE Smart Structures and Materials*, vol. In Press, 2003.

[56] Madden, J. D., Cush, R. A., Kanigan, T. S., and Hunter, I. W., Fast contracting polypyrrole actuators *Synthetic Metals*, vol. 113, pp. 185-193, May, 2000.

[57] Yamaura, M., Hagiwara, T., and Iwata, K., Enhancement of electrical conductivity of polypyrrole film by stretching: counter ion effect *Synthetic Metals*, vol. 26, pp. 209-224, 1988.

[58] Kohlman, R. S. and Epstein, A. J. Insulator-metal transistion and inhomogeneous metallic state in conducting polymers. In: *Handbook of Conducting Polymers*, eds. Skotheim, T. A., Elsenbaumer, R. L., and Reynolds, J. R. New York: Marcel Dekker, 1998.pp. 85-122.

[59] N. Vandesteeg, P. Madden, J. Madden, P. Anquetil & I. Hunter, "Synthesis and characterization of EDOT-based conducting polymer actuators", *Proceedings of SPIE*, vol. 5051, pp. 349-356, 2003.

[60] J. Madden, B. Schmid, R. Botha, M. Hechinger, S. Lafontaine, P. Madden, F. Hover, K. MacLetchie, and I. Hunter, "Polymer actuated variable camber foils", in this issue.

[61] Online content, available at: http://www.micromuscle.com.

[62] Azumi R., Goetz G. and Baeuerle P., Self-Assembly of Alkylsubstituted Oligothiophenes", *Synthetic Metals*, Vol. **101**, pp. 569-572; 1999.

[63] Brocks G., π-dimers of oligothiophene cations", *Journal of Chemical Physics*, Vol. **112**, (12): pp. 5353-5363; 2000.

[64] Graf D.D., Campbell J.P., Miller L.L. and Mann K.R., Single-Crystal X-ray Structure of the Cation Radical of 3',4'-Dibutyl-2,5"-diphenyl-2,2'-terthiophene: Definitive Evidence for π-Stacked Oxidized Oligothiophenes", *Journal of the American Chemical Society*, Vol. **118**, pp. 5480-5481; 1996.

[65] Anquetil P.A., Yu H.-h., Madden J.D., Madden P.G.., Swager T.M. and Hunter I.W.: Thiophene Based Molecular Actuators, *SPIE 9th annual symposium on electroactive materials and structures*, San Diego, CA, USA, Vol. **4695**, pp. 424-434, March 18-21; 2002

[66] Kingsborough R.P. and Swager T.M., Polythiophene Hybrids of Transition-Metal Bis(salicylidenimine)s: Correlation between Structure and Electronic Properties", *Journal of the American Chemical Society*, Vol. **121**, (38): pp. 8825-8834; 1999.

[67] Marsella M.J. and Reid R.J., Toward Molecular Muscles: Design and Synthesis of an Electrically Conducting Poly[cyclooctatetrathiophene]", *Macromolecules*, Vol. **32**, pp. 5982-5984; 1999.

[68] Marzari N. and Schleris Perel D., private communication.

[69] Sirringhaus H., Brown P.J., Friend R.H., Nielsen M.M., Bechgaard K., Langeveld-Voss B.M.W., Spierling A.J.H., Janssen R.A.J., Meijer E.W., Herwing P. and de Leeuw D.M., Two-Dimensional Charge Transport in Self-Organized, High-Mobility Conjugated Polymers", *Nature*, Vol. **401**, pp. 685-689; 1999.

[70] Yamamoto T., Kamarudin D., Arai M., Lee B.-L., Suganuma H., Asakawa N., Inoue Y., Kubota K., Sasaki S., Fukuda T. and Matsuda H., Extensive Studies of π Stacking of Poly(3-alkylthiophene-2,5-diyl)s and Poly(4-alkylthiazole-2,5-diyl)s by Optical Spectroscopy, NMR Analysis, Light Scattering Analysis, and X-ray Crystallography", *Journal of the American Chemical Society*, Vol. **120**, pp. 2047-2058; 1998.

[71] P. Anquetil, H. Yu, J. Madden, T. Swager, & I. Hunter, "Recent advances in thiophene-based molecular actuators", *Proceedings of the SPIE*, vol. 5051, pp. 42-53, 2003.

[72] Ray H. Baughman, Cui Chanxing, Anvar A. Zakhidov, Zafar Iqbal, Joseph N Barisci, Geoff M. Spinks, Gordon G. Wallace, Alberto Mazzoldi, Danilo De Rossi, Andrew G Rinzler, Oliver Jaschinski, Siegmar Roth, Miklos Kertesz, "Carbon nanotube actuators", Science 284, 1999, pp. 1340-1344.

[73] J.N. Barisci, G.G. Wallace and, G. Spinks, "Electrochemical Characterization of Single-Walled Carbon Nanotube Electrodes." Journal of the electrochemical society 147, 2000, p. 4580.

[74] G. Gu, M. Schmid, P.-W. Chiu, A. Minett, J. Fraysee, G.-T. Kim, S. Roth, M. Kozlov, E. Munoz & R. Baughman, "V_2O_5 nanofibre sheet actuators", *Nature Materials*, vol. 2, pp. 316-319, 2003.

[75] Kim, K.J., Shahinpoor, M. *Polymer* 43 (2002) 797-802

[76] Shahinpoor, M. Kim, K.J. *Sensors and Actuators A* 96 (2002) 125-132

[77] Nemat-Nasser, S. *Journal of Applied Physics* 92, 5 (2002) 2899-2915

[78] Nemat-Nasser, S., Wu, Y. *Journal of Applied Physics* 93, 9 (2003) 5255-5267

[79] Shahinpoor, M., Kim, K.J. *Smart Mater. Struct.* 10 (2001) 819-833

[80] Shahinpoor, M., Kim, K.J. *Smart Mater. Struct.* 9 (2000) 543-551

[81] Noh, T., Tak, Y., Nam, J., Choi., H. *Electrochimica Acta* 47 (2002) 2341_2346

[82] Online content available at: Biomimetic Products Inc. http://www.biomimetic.com/, 2003.

[83] A. E. Clark, *Ferromagnetic Materials* vol 1, ed E P Wohlfarth (North-Holland, Amsterdam, 1980) p. 531.

[84] A. E. Clark, *AIP Conf. Proc. 18* (American Institute of Physics, New York, 1974) p. 1015.

[85] Online content available at: http://www.etrema-usa.com, 2003.

[86] D. C. Jiles, *Introduction to Magnetism and Magnetic Materials* (Chapman and Hall, New York, 1991).

[87] R. C. Smith, M. J. Dapino, S. Seelecke, J. Appl. Phys. **93**, 458 (2003).

[88] A. E. Clark, *MRS Symp. Proc. 360* (Materials Research Society, Pennsylvania, 1994) p. 171.

[89] H. Janocha, Sensors and Actuators A **91**, 126 (2001).

[90] D. C. Jiles, J. Phys. D: Appl. Phys. **27** 1 (1994).

[91] X. Zhao, G. Wu, J. Wang, K. Jia, W. Zhan, J. Appl. Phys. **79** 6225 (1996).

[92] F. Claeyssen, N. Lhermet, R. Le Letty, P. Bouchilloux, J. Alloys and Compounds **258**, 61 (1997).

[93] L. Sandlund, M. Fahlander, T. Cedell, A.E. Clark, J. B. Restroff, M. Wun-Fogle, J. Appl. Phys. **75** 5656 (1994).

[94] M. J. Sablik and D. C. Jiles, IEEE Transactions on Magnetics **29**, 2113 (1993).
[95] Basinski, Z.S. and Christian, T. Acta Metallurgica, 1954, 2, 101.
[96] Bergamasco, M. Salsedo, F. and Dario, P. A linear SMA motor as direct-drive robotic actuator. 1989 IEEE International Conference on Robotics and Automation, May, 1989, Scottsdale, Arizona, 618-623.
[97] Bergamasco, M. Salsedo, F. and Dario, P. Shape memory alloy micro-motors for direct-drive activation of dexterous artificial hands. Sensors and Actuators, 1989, 17, 115-119.
[98] Buehler, W.J., Gilfrich, J. and Wiley, K. Journal of Applied Physics, 1963, 34, 1465.
[99] Chang, L.C. and Read, T.A. Transactions of the American Institute of Mechanical Engineers, 1951, 189, 47.
[100] Delaey, L., Thienel, J. Shape Memory Effects in Alloys, Jeff Perkins (Ed), Plenum, 1975, New York, 341-350.
[101] Funakubo, H. (ed.) Shape Memory Alloys. Gordon and Breach: New York, 1987.
[102] Hirose, S., Ikuta, K. and Umetani, Y. A new design method of servo-actuators based on the shape memory effect, in Theory and Practice of Robots and Manipulators, Proceedings of RoManSy'84, the 5th CISM-IFToMM Symposium, Hermes Publishing, 1985, 339-349.
[103] Hirose S., Ikuta, K. and Sato, K. Development of a shape memory alloy actuator. Improvement of output performance by the introduction of a s-mechanism. Advanced Robotics, 1989, 3, 89-108.
[104] Homma, D., Miwa, Y. and Iguchi, N. Micro robots and micro mechanisms using shape memory alloy. The 3rd Toyota Conference Integrated Micro Motion Systems: Micromachining, Control and Application. Nissin, Aichi, Japan, October, 1989, 22, 1-21.
[105] Hunter, I.W. Novel Actuators For Use in Robotics And Tele-Robotics, Report Prepared for the US Office of Naval Research, 1990, 88p.
[106] Hunter, I.W., Lafontaine, S. and Hollerbach, J.M. Artificial muscle prototype for use in robotic and prosthetic limbs. Proceedings of the 16th Canadian Medical and Biological Engineering Conference, 1990, 16, 35-36.
[107] Hunter, I.W., Lafontaine, S., Hollerbach, J.M. and Hunter, P.J. Fast reversible NiTi fibers for use in microrobotics. Proceedings IEEE Micro Electro Mechanical Systems, 1991, 2, 166-170.
[108] Ikuta, K. Micro/miniature shape memory alloy actuator. Proceedings IEEE Micro Electro Mechanical Systems, 1990, 3, 2156-2161.
[109] McCormick, P.G., On the practical efficiency of shape memory engines, Scipta Metallugica 1987 21, 99-101.
[110] Otsuka, K. and Shimizu, K. Scripta Metallurgica, 1970, 4, 469.
[111] Van Humbeeck, J., Chandrasekaran, M. and Delaey, L. Shape memory alloys: materials in action. Endeavour, New Series, 1991a, 15(4), 147-154.
[112] V. A. Chernenko, E. Cesari, V. V. Kokorin, I. N. Vitenko. "The Development of New Ferromagnetic Shape Memory Alloys in Ni-Mn-Ga System." *Scripta Metallurgica et Materialis* **33**, pp. 1239-1244 (1995).
[113] K. Ullakko, J. K. Huang, C. Kantner, R. C. O'Handley, V. V. Kokorin. "Large magnetic-field-induced strains in Ni_2MnGa single crystals." *Appl. Phys. Lett.* **69**, pp. 1966-1968 (1996).
[114] A. N. Vasil'ev, A. D. Bozhko, V. V. Khovailo, I. E. Dikshtein, V. G. Shavrov, V. D. Buchelnikov, M. Matsumoto, S. Suzuki, T. Takagi, J. Tani. "Structural and magnetic phase transitions in shape-memory alloys $Ni_{2+x}Mn_{1-x}Ga$." *Phys. Rev. B* **59**, pp. 1113-1120 (1999).
[115] S. J. Murray, M. Marioni, S. M. Allen, R. C. O'Handley, T. A. Lograsso. "6% magnetic-field-induced strain by twin-boundary motion in ferromagnetic Ni-Mn-Ga." *Appl. Phys. Lett.* **77**, pp.886-888 (2000).
[116] A. Sozinov, A. A. Likhachev, N. Lanska, K. Ullakko. "Giant magnetic-field-induced strain in NiMnGa seven-layered martensitic phase." *Appl. Phys. Lett.* **80** pp.1746-1748 (2002).
[117] S. J. Murray, M. A. Marioni, A. M. Kukla, J. Robinson, R. C. O'Handley, S. M. Allen. "Large field indsuced strain in single crystalline Ni-Mn-Ga ferromagnetic shape memory alloy." *J. Appl. Phys.* **87**, pp. 5774-5776 (2000).
[118] R. Tickle, R. D. James, T. Shield, M. Wuttig, V. V. Kokorin. "Ferromagnetic Shape Memory in the NiMnGa System." *IEEE Trans. Magnet.* **35**, pp.4301-4310 (1999).
[119] R. Tickle, R. D. James. "Magnetic and magnetomechanical properties of Ni_2MnGa." *J. Magn. Magn. Mater.* **195**, pp.627-638 (1999).
[120] R. C. O'Handley, S. J. Murray, M. Marioni, H. Nembach, S. M. Allen. "Phenomenology of giant magnetic-field-induced strain in ferromagnetic shape-memory materials" *J. Appl. Phys.* **87**, pp.4712-4717 (2000).
[121] M. A. Marioni, R. C. O'Handley, S. M. Allen. "Analytical model for field-induced strain in ferromagnetic shape-memory alloy polycrystals." *J. Appl. Phys.* **91**, pp.7807-7809 (2002).
[122] Online content available at: http://www.adaptamat.com , 2003.
[123] C. Jiang, T. Liang, H. Xu, M. Zhang, G. Wu. "Superhigh strains by variant reorientation in the nonmodulated ferromagnetic NiMnGa alloys." *Appl. Phys. Lett.* **81**, pp.2818-2820 (2002).
[124] S. Murray, Report to Darpa by Mide Corporation, "Ferromagnetic Shape Memory Alloys: Device Applications", http://www.darpa.mil/dso/thrust/matdev/chap/briefings/timchap2000day3/murray_mide.pdf, 2000.
[125] K. MacLetchie et. al., included in this publication.

ACKNOWLEDGMENT

This project was conceived by Dr. Promode Bandyopadhyay and Dr. Harold Bright at ONR. Many thanks to Franzi Tschurtschenthaler for assistance with dielectric elastomer figures of merit